# EFFECT OF VERY SLOW DRYING, DCCA'S AND PREHYDROLYSIS ON THE STRENGTH OF SOL-GEL PREPARED PZT FIBRES

A Thesis Submitted

in Partial Fulfillment of the Requirements

for the Degree of

MASTER OF TECHNOLOGY

by

SOUMEN ROY
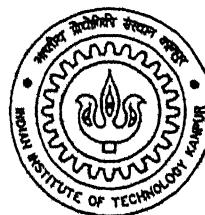
to the

MATERIALS SCIENCE PROGRAMME

INDIAN INSTITUTE OF TECHNOLOGY KANPUR

March, 1998
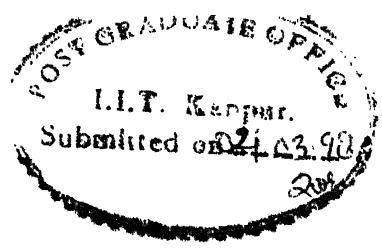
CERTIFICATE

It is certified that the work contained in the thesis entitled " **Effect of very slow drying, DCCA's and prehydrolysis on the strength of sol-gel prepared PZT fibres** ", *by* **Soumen Roy**, has been carried under my supervision and that this work has not been submitted elsewhere for a degree.

3.3.98

Prof. D.C. Agrawal

Materials Science Programme

I.I.T., Kanpur

March, 1998.

DEDICATED TO

Ma   O   Baba

Acknowledgement

Abstract

Lead Zirconate Titanate (PZT) ceramic fibres prepared by sol-gel process have very low strength. This makes them unsuitable for use in applications such as transducers etc. In this work PZT fibres were prepared by the sol-gel process and an attempt was made to investigate the causes of their low strength. The fibres and the gel from which they were derived were characterized with various techniques such as X-ray diffraction, scanning electron microscopy, thermogravimetric analysis, differential thermal analysis and strength measurements. Drying cracks were found to be present in the as prepared PZT fibres. The effect of very slow drying of the as drawn fibres, adding different amount of water to the sol to form particles and of adding drying control chemical additives (DCCA) such as DMF and formamide on the formation of cracks in the fibres was studied. The sintered fibres showed different microstructures depending on the processes used. The strength of the fibres measured by three point bending method and analysed by Weibull approach reveals different strength value for the various preparation methods. The fibres made without any additives were too fragile for measurement of strength. Addition of DCCA's improves the strength. A nominal strength of 40 MPa is obtained upon addition of small amounts of formamide. Increasing the amount of formamide leads to a lowering of strength. Strength values, ranging from 50 to 80 MPa are obtained when DMF is used. The PZT fibres prepared with PEG-400 have cracks in the cross-section of the fibres in the as prepared state, but these cracks heal after sintering the fibres giving a dense microstructure. These fibres have the highest strength giving upto $\sim$ 90 MPa. However, these strength values are still an order of magnitude lower than the strength of about 1 GPa obtained in other ceramic fibres.

Contents

List of Figures

List of Tables

Chapter 1

Introduction

1.1 Ceramic Fibres

During the last quarter of the century, great progress has been made in the develoopement of high-performance materials. One of the major areas in the progress has been the production of inorganic or ceramic fibres. These fibres with their high tensile strength and modulus and their resistance to high temperature have become very useful for reinforcing ceramics, polymers and metals. The composites thus produced, have superior properties and are already in use for the construction of space vehicles, sports goods, lightweight structures and various other engineering equipments. Work is also being carried out to make fibres from electronic ceramics for their potential applications in electronic control systems, smart structures and various other sensors.

The first important inorganic fibres made were asbestos and glass. After that much reserch has been done and many new high-performance inorganic fibres have resulted. These include silicon carbide(SiC), silicon nitride(Si_3N_4), boron, carbon, titania, zirconia and many others, some in whisker and some in polycrystalline form. These fibres are light in weight and have high strength and modulii, but are usually very costly to produce. These fibres find use in composites with metal, ceramic or polymer matrix. The patent list in the field of inorganic fibres and composites containing these fibres is extensive [1].

1.2 Methods of making ceramic fibres

The strength of inorganic fibres greatly depends on the microstructure [2]. Pores, defects, as well as crystallite size markedly affect the microstructure and hence the

Table 1.1: Influence of diameter on tensile strength of glass fibres [3]

Diameter (μ m)	Ultimate tensile strength(GPa)
19.0	0.7
15.2	0.9
12.7	1.0
10.2	1.3
8.6	1.7
5.1	2.8
2.5	6.0

properties. Table 1.1 shows the influence of diameter on tensile strength of glass fibres [3]. The values show a decrease in strength with an increase in fibre diameter. This is due to the fact that there are fewer imperfections and faults as the fiber diameter is reduced.

The microstructure and the fibre strength are strongly influenced by the method used to produce the fibres. So suitable manufacturing process is to be adopted. some of the important processes developed during the 70's and afterwards are briefly reveiwed below.

A. Melt Spinning

The raw material is melted and then made into fibres in one of the two ways.

(1) This method called 'blown process', involves pouring the molten material into the path of a high velocity blast from a stream of compressed air, which shreds the molten oxide into small droplets. The droplets elongate and attenuate into a fibre.

(2) In the other method, called the 'spun process', the molten material is fed onto a vertically oriented, rapidly rotating disk from which fibres are thrown by centrifugal force.

B. Slurry Process

This process, developed particularly for Al_2O_3 fibres, involves extruding slurries of Al_2O_3 or Al_2O_3 hydrate particles, and drying and heating the resulting fibres to produce polycrystalline filament [3]. Fiber FP (trade name) an alumina-silica fiber, is manufactured by this process by E.I. du pont, USA.

C. Solution Process

It involves extruding and drawing into fibres of a viscous solution of the compounds, followed by drying and heating the resulting fiber at high temperatures. The process has been used to make Nextel fibres containing Al_2O_3, SiO_2 and B_2O_3 by 3M corporation, USA.

D. Vapour-deposition Process

This process is mainly used to prepare boron fibres by coating boron onto a tungsten core or carbon fibres, using vapour-deposition technique.

E. Relic Process

Union carbide uses this process for the preparation of metal oxide fabrics [US patent No. 3663182]. Organic fibres or fabrics are impregnated with metal oxide precursors. Subsequent controlled heating results in formation of oxide fibres or fabrics.

Another important process for making ceramic fibres is the sol-gel process which is described in the next section.

1.3 Ceramic Fibres by Sol-Gel Process

Sol-gel process as described later is especially useful for the preparation of inorganic fibres because of its low temperature processing, simplicity and homogenity of the product formed. Before the use of sol-gel process ceramic fibres were generally prepared from fused oxides, this requires high temperature and also viscoelastic properties of the melt. Compositions were limited to fibres containing high percentage of silica [4].

A wide range of oxide and non oxide fibres are prepared by sol-gel process starting from polymeric or polymerizable sources, such as alkoxides. Two main processes of preparing ceramic fibres from sol-gel process are drawing fibres directly from the viscous sol at room temperature, and unidirectional freezing of gels in which a hydrogel is placed in a polyethylene cylinder that is slowly lowered into a bath of liquid nitrogen. The gel is frozen after which the cylinder is removed at room temperature to form the fibres. A wide range of gel derived ceramic fibres available commercially are listed in table 1.2

Ceramic fibres of SiO_2, ZrO_2, TiO_2 and their combination are also developed with strength reaching upto 1000 MPa. The synthesis of zirconia fibre is reported by T.Yogo [5]. Maschio et al. reported a strength upto 1200 MPa for SiO_2-ZrO_2 fibres [6]. Fibres

Table 1.2: Commercially available ceramic fibres.

Producer	Name	Composition	Tensile Strength (MPa)	Tensile Modulus (GPa)	Density (gm/cm^3)
3M	Nextel 312	Al_2O_3,SiO_2,B_2O_3	1750	154	2.70
3M	Nextel 440	Al_2O_3,SiO_2,B_2O_3	2100	189	3.05
3M	Nextel 480	Al_2O_3,SiO_2,B_2O_3	2275	224	3.05
du Pont	PRD-166	Al_2O_3,ZrO_2	2100	385	4.20
du pont	FP	alpha Al_2O_3	1400	3835	3.90
Sumitomo		Al_2O_3,SiO_2	av. 2200	av. 230	3.20

of SiO_2-TiO_2 with strength of magnitude 1 GPa have been reported by Murlidharan and Agrawal [7].

1.4 The Sol-Gel process

Sol-gel process begins with a colloidal dispersion, or sol, of particles or polymers in a liquid. Through subsequent chemical cross-linking and evaporation, the fluid sol is transformed into a rigid gel, which is a substance containing a continuous solid skeleton enclosing a continuous liquid phase. This sol to gel transition allows the solid phase to be shaped into fibres, films or monoliths.

The main advantage gained by sol-gel processing is the ability to control both the composition and microstructure, including density, refractive index, pore size and surface area, usually on molecular length scale [17].

1.4.1 Chemistry of Sol-Gel Processing

The sol to gel transition is characterised by two fundamental reactions i.e, hydrolysis and condensation as described below.

Hydrolysis

Metal alkoxides are generally very reactive chemicals. They are extremely succeptiable to hydrolysis by atmospheric moisture. The reaction is illustrated below taking the well studied silicon alkoxide (tetra ethyl ortho silicate) $Si(OC_2H_5)_4$.

4

OR
|
RO —— Si —— OR + H_2O ⟶ RO —— Si—— OH + ROH
| |
OR   OR

or,

| |
—— M —— OR + H —— O ⟶ —— M —— OH + ROH
| | |
                                H
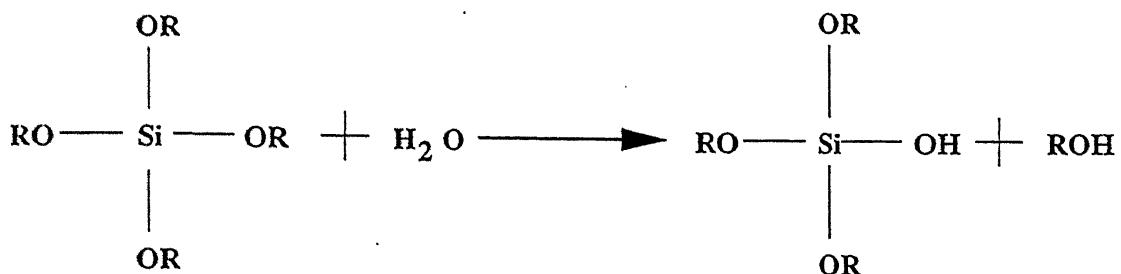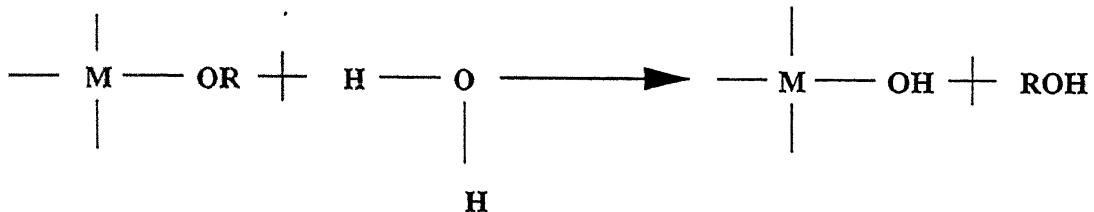
The hydrolysis reaction

Condensation

Condensation starts before a molecule is fully hydrolysed. It generally occurs in two ways, either by the removal of alcohol (alcoxolation) or water (oxolation). The reactions are shown in the next page.

Role of catalyst

Acid or base catalysts can influence both the hydrolysis and condensation rates and the structure of the condensed product. Acids serve to protonate negatively charged alkoxide groups. The reaction can be expressed by the following equation,

$$[OR]_3 Si - OR + H_3O^+ \longrightarrow [RO]_3 SiOH + H^+ + HOR$$

$$H^+ + H_2O \longrightarrow H_3O^+$$
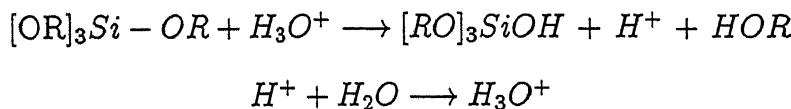
In base catalyzed hydrolysis, a nucleophilic substitution of hydroxy ions for OR grops occurs. The reaction is shown in the following equation,

$$[RO]_3 SiOR + OH^- \longrightarrow [RO]_3 SiOH + OR^-$$

$$OR^- + H_2O \longrightarrow HOR + OH^-$$

OR
|
RO—Si—OH + OH—Si—OR ⟶ RO—Si—O—Si—OR
| | | |
OR   OR   OR   OR

OR   OR   OR   OR

(Oxolation) $+$ H_2O

OR   OR   OR   OR
| | | |
RO—Si—OH + RO—Si—OR ⟶ RO—Si—O—Si—OR
| | | |
OR   OR   OR   OR

(Alkoxolation) $+$ ROH
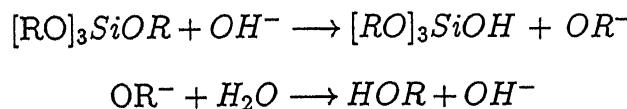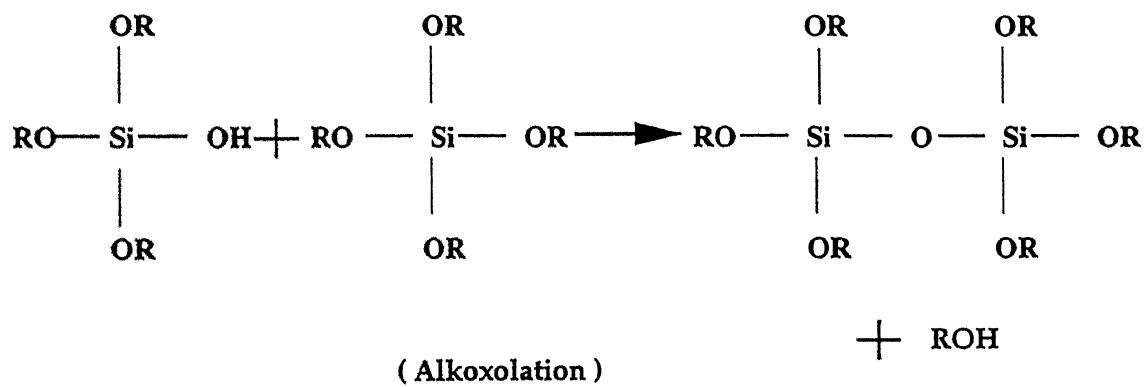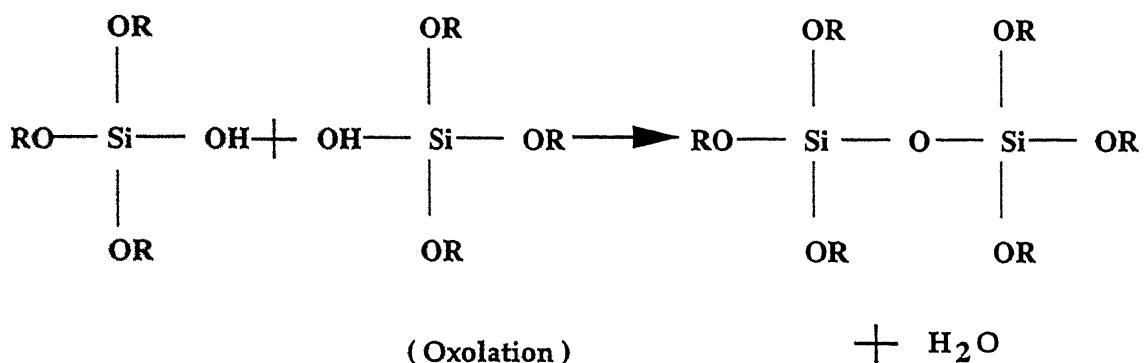
The condensation reaction for silicon alkoxide.

R represents an alkyl group.

1.4.2 Factors affecting the Sol-Gel process

The main parameters affecting the sol-gel process are,

(1) Precursors (2) Reaction conditions (3) Mechanical parameters.

Precursors

The rate of hydrolysis reaction depends on the nature of the precursor used to prepare the sol i.e, salts, oxides, alkoxides or colloids. The metal alkoxides are the most reactive species.

Reaction conditions

The reaction mechanism of sol-gel process is affected by solvent, temperature, catalyst. PH and water content.

Solvents

The solvents that are commonly used in the sol-gel process are the alcohols. These alcohols have relatively high vapour pressure even at room temperature. The solvent loss due to evaporation is a major factor causing gelation of the sol. These solvents which remains in the pores of the wet gel play an important part in the drying process.

Temperature

The gelation time becomes shorter as the sol-gel reaction temperature becomes higher. It has been shown by Colly et. al [9] that the following Arrhenius relationship is obeyed,

$$\frac{1}{t_g} = A.exp[-\frac{E^*}{R.T}] \tag{1.1}$$

Where,
t_g = Gelation time.
E^* = Activation energy.
T = Temperature.
A , R = Constants.

Water content

Water is directly involved in the chemical reactions that form the molecular structure. SAKKA et al [10] observed that a large water content favours the formation of non-linear or network polymers in the hydrolysis of $Si[OC_2H_5]_4$. The aggregation of

these polymers results in the increase in viscosity of the sol. It is supposed that this gives the solution an elastic nature, which prohibits the occurance of spinnability.

Mode of Reaction

The gelation time strongly depends on the system in which the reaction takes place i.e. open or close or partially open system. In the open system the time is much smaller as the vaporization of reaction products such as alcohol and water increases the rate of reaction.

Mechanical Parameters

The gelation time, particle size, agglomeration are affected by mechanical parameters like stirring, ultrasonication and refluxing.

1.4.3 Precursors of Sol-Gel Process

Metal alkoxides are widely used as sol-gel precursor for synthesis of metal oxides. These alkoxide sols upon hydrolysis and condensation form gel which gets converted into high purity oxides after heat treatment at moderate temperature. In general a metal alkoxide has the chemical formula $M(OR)_n$, where M is the metal atom and R is the alkyl group such as methyl (CH_3), ethyl (C_2H_5), propyl (C_3H_7), butyl(C_4H_9) etc. The alkyl group has a strong influence on rate of hydrolysis which is more rapid with methyl group and reduces as one goes to higher alkyls.

1.4.4 Aging of Gels

Polymerization, coarsening and phase transformation marks the aging process. The condensation reactions that bring about gelation also result in progressive strengthening and stiffening of the gel during aging. The process depends on such factors as PH, temperature and composition of the solution. In liquids in which the solid phase is soluble, dissolution and reprecipitation process causes coarsening as material is transported to surface of lower curvature. This results in loss of micropores, decrease in surface area, and stiffening through growth of interparticle necks. Figure 1.1 shows the neck formation where two particles of radius R is joined by a neck with radius X. The radius of curvature of the neck, r, is determined by the solubility of the solid, so it varies with temperature and PH [7].

8
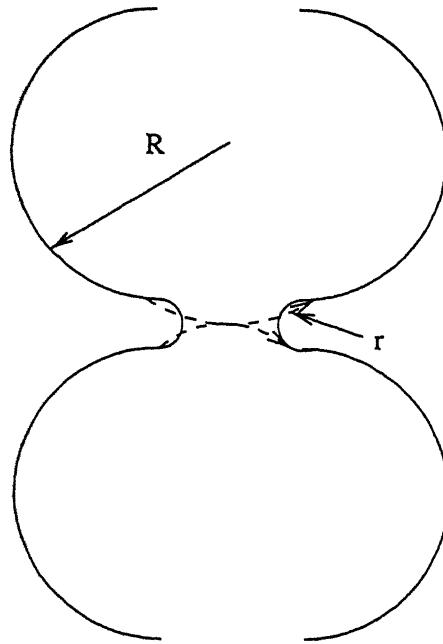
Figure 1.1: Neck formation in particles

1.4.5 Drying of Gels

Drying of gels is important for fibres and films as these may lead to cracking. Gels consist of large number of nanosized pores with non-uniform distribution. These pores have trapped solvent in them. During drying, shrinkage occurs causing non uniform capillary stresses which result in cracking of the gel. There are different methods to control the cracking. In view of its importance a brief description of the theory of drying and the different methods used to control the drying cracks are given in the following section.

1.4.5.1 Theory of Drying

The process of drying of porous material can be divided into four stages - constant rate period (CRP), critical point (CP), first falling rate period (FRP1), and second falling rate period (FRP2). The rate of evaporation during these periods can be understood from figure 1.2 [11], showing the water loss from alumina gel. The critical point during which the stress in gel is maximum is the end of CRP and starting of FRP1.

The schematic representation of the stages of drying is shown in figure 1.3 [11]. At the onset of drying, the surface of the liquid is flat. The curvature increases as the liquid of the gel evaporates. The liquid is then in tension, and as a consequence the

9
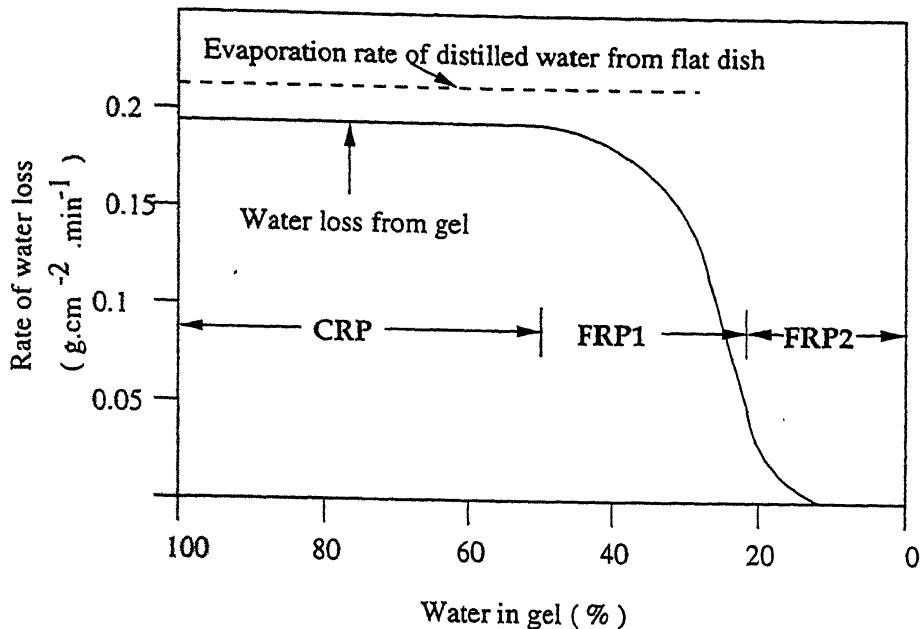
Figure 1.2: Rate of water loss from alumina gel [11]

solid part of the gel is under compression. This effect causes the gel network to shrink. The shrinkage continues as long as the solid network (depending on the nature of the gel) is not stiff enough to resist the compressive stress.

The relation between pressure gradient and evaporation rate has been shown by Brinker Scherer [11] to be

$$\nabla P_{surface} = \frac{\dot{E}_v.\eta_l}{D} \qquad (1.2)$$

Where,

∇P = Pressure gradient in gel.

$\dot{E}_v$ = Rate of evaporation of liquid from gel.

η_l = Liquid viscosity.

D = Permeability of gel.

It is the pressure gradient caused by low gel permeability that causes differential strain and cracking. It is calculated by Brinker and Scherer [11] that for alkoxide derived gel, the capillary stress may be in the order of 3-200 MPa. This stress is large enough to cause cracks in the gel body. There are different methods used to control the drying cracks illustrated in the next section.

10

a) Initial condition

Liquid / vapor meniscus flat

Pore liquid

Solid phase

b) Constant rate period

r

Evaporation
⟶
Shrinkage

r

c) Falling rate period

Maximum capillary pressure:

$$P_R = \frac{(\gamma_{SV} - \gamma_{SL}) S_p}{V_p}$$

Empty pores

Minimum radius of curvature
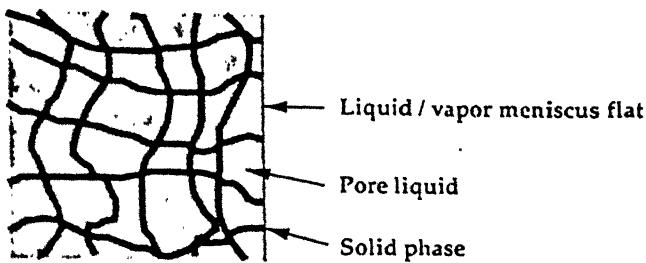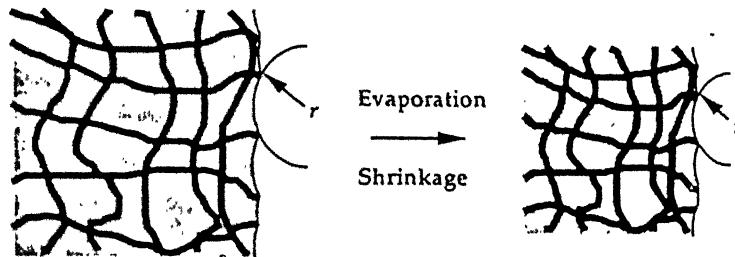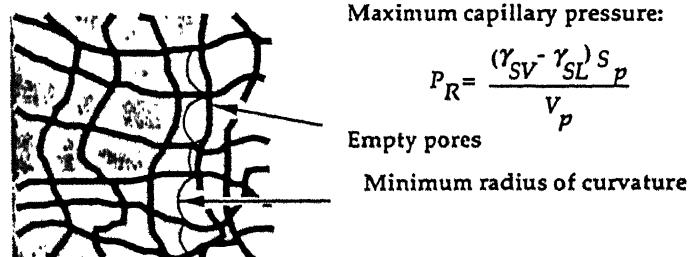
Schematic illustration of drying process. Capillary tension developes as liquid flows to prevent exposure of the solid phase by evaporation, and the network is drawn back into liquid. Initially the network is so compliant that little stress is needed to keep it submerged, so the tension in the liquid is low and the radius of the meniscus (r) is large. (b) As the network stiffens, the tension rises and r decreases. At the critical point, the radius of the meniscus becomes equal to the pore radius; then the CRP ends and the liquid recedes into the gel (c). [Ref. 11]

Figure 1.3: Stages of drying

1.4.6 Methods of Controlling Drying cracks

The different methods used to control the drying cracks in the gel are listed below and are then briefly described.

- Slow Evaporation Rate.

- Supercritical Drying.

- Larger Pores

- Aging for longer time

- Use of chemical additives:
  Surfactants, Drying Control Chemical Additives and Plasticizer.

1.4.6.1 Slow Evaporation Rate

As described in the last section, it is the pressure gradient that is responsible for the drying cracks in the gel. The relation between the rate of evaporation and pressure gradient is given by equation 1.2. It is clear from the equation that a slower evaporation rate will cause a lower pressure gradient, Thus the possibility of cracking will decrease. The rate of evaporation of solvent from the gel can be controlled by controlling the ambient atmosphere and pressure.

1.4.6.2 Supercritical Drying

Since shrinkage and cracking are produced by capillary forces, these problems can be avoided by removing the liquid from the pores above the critical temperature (T_c) and critical pressure (P_c) of the liquid. Figure 1.4 shows the liquid-vapour phase boundary (dark curve) and the critical point (T_c, P_c). At the critical point the densities of the liquid and vapour phase become equal so that there is no liquid-vapour interface and no capillary pressure.

In the process, the wet gel is placed into an autoclave and heated along path shown as (A) in figure 1.4 in such a way that the phase boundary is not crossed. The pure liquid is generally exchanged with a suitable solvent with lower T_c and P_c. The critical points of some selected solvents are shown in table 1.3.
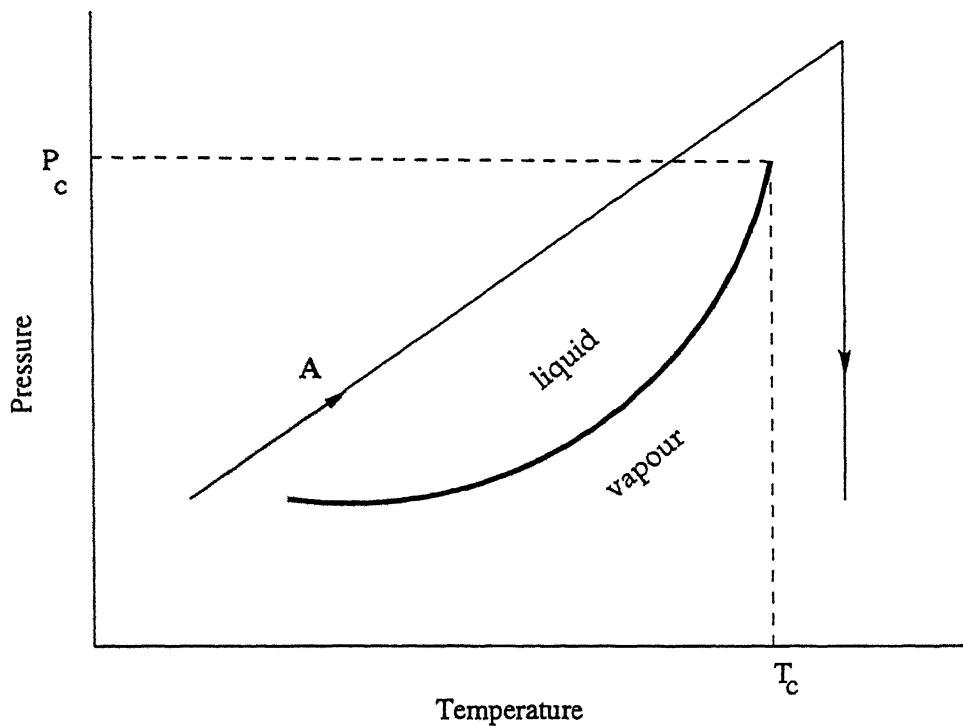
Figure 1.4: Critical point And Supercritical Drying Route

Table 1.3: Critical point of some solvents

Substance	Formula	$T_c(^oC)$	$P_c(MPa)$
Carbon Dioxide	CO_2	31.1	7.36
Freon 116	CF_3CF_3	19.7	2.97
Methanol	CH_3OH	240	7.93
Ethanol	C_2H_5OH	243	6.36
Water	H_2O	374	22.0

1.4.6.3 Larger Pores

The relation between tension P in the pore liquid during drying with the radius of pores a, is given by [7],

$$P = \frac{2\gamma_{lv} Cos\theta}{a} \qquad (1.3)$$

where, γ_{lv} is the liquid-vapour interfacial energy and θ is the contact angle between the solid and liquid phase. From the above equation it is clear that the capillary tension in the pore liquid during drying and thus the probability of cracking of the gel can be reduced by increasing size of the pores present in the gel. However the resulting body needs to be sintered at higher temperatures. Larger pore size also results in increased permeability of the gel thus reducing the pressure gradient developed during drying.

The pore size is generally increased by washing in an acid (HF) or basic medium. Another method is to add fillers to the gel. Fumed silica, stobler silica particles and ludox (a colloidal silica solution) are the fillers most often used for silica gel. Fillers decrease shrinkage during drying and prevent the collapse of pores.

1.4.6.4 Aging for longer time

Aging a gel for longer time before drying increases the gel connectivity therby strengthening the network [12]. Thus the chance of fracture in the gel gets reduced. This is proved by measuring the modulus of rupture and stress intensity factor of gels subjected to various period of aging in their own pore liquid [13].

1.4.6.5 Chemical Additives

Surfactants are added with the pore liquid to reduce interfacial energy, thus decreasing the capillary stress as is evident from equation 1.3. It is shown [22] that for alkoxide derived gels, cracking is reduced by surfactants.

Drying control chemical additives (DCCA) are a group of chemicals which can be used for faster drying of wet gel without cracking. There are two types of DCCA - acidic DCCA such as oxalic acid, and basic DCCA such as formamide, dimethyl formamide (DMF) etc. Addition of basic DCCA produces a large sol-gel network with uniformly larger pores whereas acidic DCCA results in a somewhat smaller scale network after gelation but also with a narrower distribution of pores [8]. The pore size distribution results in greater permiability of the gel and less capillary pressure thus controlling the cracking in the gel [15,18]. This ultrastructural control is due to DCCA's effect on the

rates of both hydrolysis and polycondensation [26]. Acid catalysis of the formamide-tetra methoxy ortho silicate (TMOS) system increases the hydrolysis rate and a rapid siloxane bond forms.

It is reported that acid catalysis together with formamide results in a 3.5 times faster rate of hydrolysis [8] . The subsequent condensation reaction has a smaller rate for acid catalyzed formamide sol than basic or neutral sol with formamide.

Another type of chemical additive used is called "plasticizer" like glycerol, polyethylene glycol etc. It reduces the capillary pressure by forming a film on the surface, thus reducing the contact angle and also due to its low vapour pressure it does not evaporate but is retained in the smallest pores. It is removed only when heated to high temperature.

1.5   Rheology of Sols and Fiber Drawing

The viscosity behaviour of the metal alkoxide sols due to hydrolysis and condensation reactions that leads to gelation is responsible for the resulting fibres and their cross-section. The rheological properties of sols leading to fibers are extensively studied by SAKKA and KOZUKA [14]. The important points are noted below:

- The viscosity of sols increases gradually until they gel at viscosity higher than 100 Poise depending on the composition of starting solution.

- When a metal alkoxide solution is catalysed with an acid and its water content is small at less than 4 or 5 in water to alkoxide molar ratio, the solution exhibits spinnability at viscosities about 10 Poise and becomes drawable into gel fibers, whereas no spinnability appears when a solution contains a large amount of water or is catalysed with an alkali like ammonia.

- Spinnable silicon alkoxide solutions have long shaped siloxane particles and non-spinnable solutions have round particles.

- Spinnable solutions exhibit Newtonian flow behaviour upto high viscosities where fibers can be drawn, while non-spinnable solutions exhibit marked structural viscosities and sometimes thixotropy.

- The gelation time depends strongly on temperature.

The variation of the viscosity of a drawable $Si(OC_2H_5)_4$ solution with the molar ratio $[H_2O]/[Si(OC_2H_5)_4] = 2$ at 25, 30 and 80^oC as a function of time is shown in

15
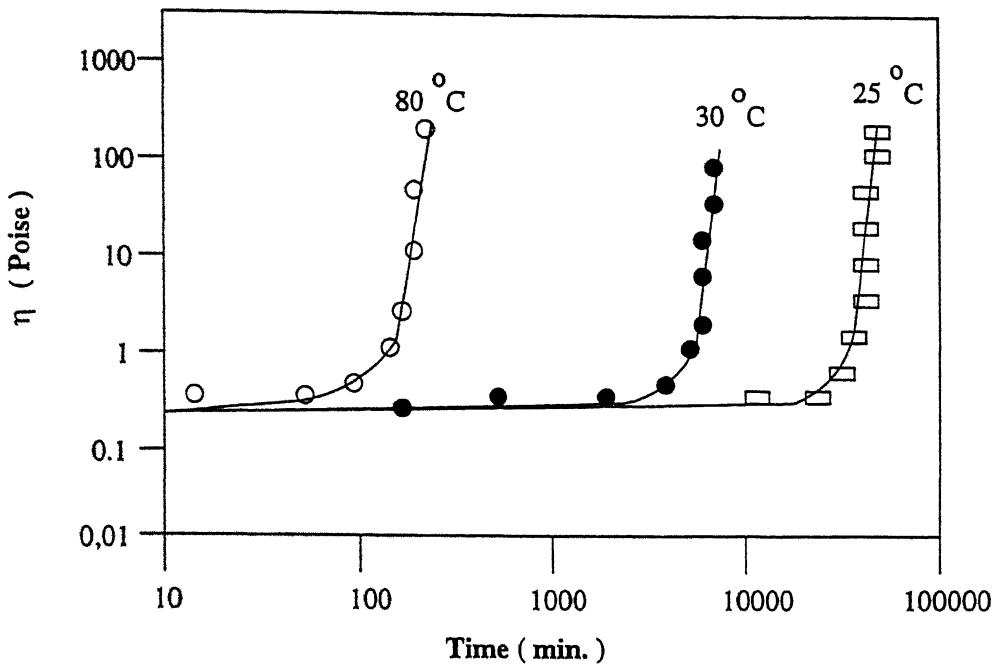
Figure 1.5: Change in viscosity for silica sol (after Sakka et al.[14])

figure 1.5. When the viscosity reaches about 10P, the solution becomes sticky and spinnable, which makes it possible to draw fibres.

1.6 Heat Treatment of Gel

After drying, the gel contains residual organics and also trapped solvent in the pores. Further densification of the gel takes place during heat treatment. First the organics get removed after which the sintering process or densification of the gel starts. Due to the small pore size in the gel [in the order of 2 to 10 nm] they densify faster than bodies made using conventially crushed powder [11].

1.7 Cracks Occuring During Heat Traetment

The thermal treatment of gel is to be carried out with care. At low temperatures the gel, which contains unreacted organic groups, must be gently oxidized. This treatment is often performed in air ambient, but long chain residues require long treatments under oxygen to achieve full oxidation. The released gas contains CO_2, H_2O, CO and some low molecular weight organics [11]. The escape of gas by-product is hindered by the low

16

permeability of the gel. The produced gas cannot escape easily. Its pressure increases, and thus the gel expands. A fast heating rate can lead to the cracking of the gel. To avoid this phenomenon, the heat treatment shedule must be optimized.
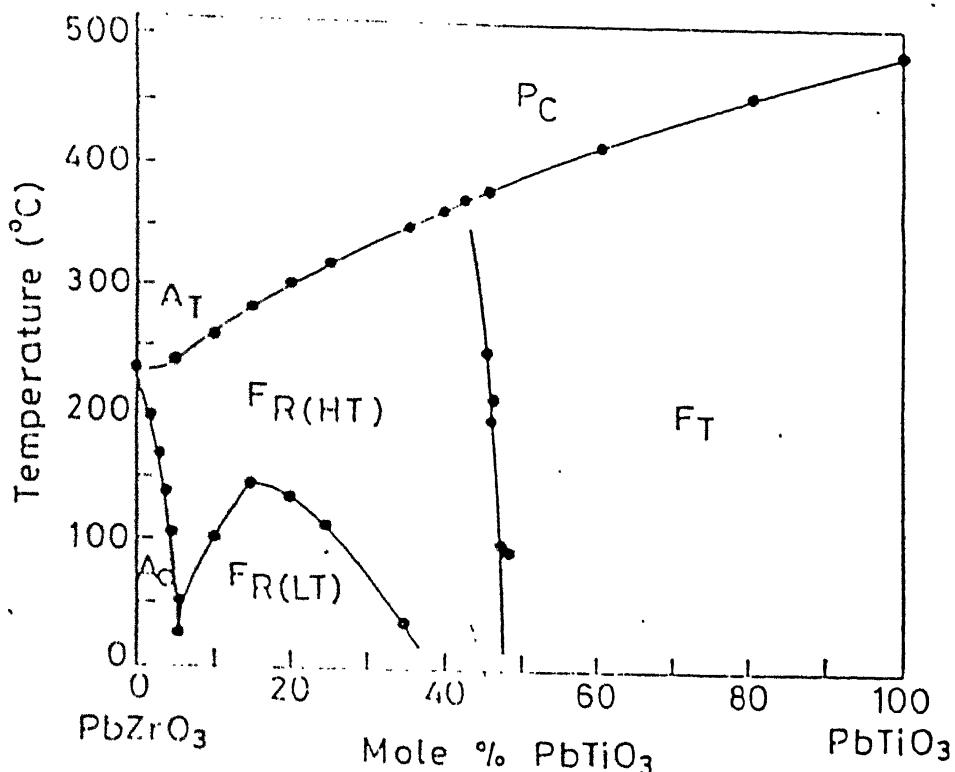
Figure 1.6: The PZT phase diagram (after Jaffe et al. [16]

1.8 Lead zirconate titanate (PZT) ceramics and fibres

The PZT ceramics are mainly used for piezoelectric applications. They, are chemically represented by $Pb(Zr_x Ti_{1-x})O_3$ and are solid solutions of lead zirconate (PZ) and lead titanate (PT). Depending on the value of x it may exist in pervoskite, tetragonal or rombohedral phase which are ferroelectric, or orthorombic phase which is antiferroelectric. At x = 0.53 the boundary between the tetragonal and rhombohedral phase exists (Figure 1.6 shows the phase diagram of PZ and PT). It denotes an abrupt structural change with composition at the same temperature. This sharp phase boundary is called morphotropic phase boundary (MPB) and the composition in this region is of great technological interest because of high value of piezoelectric coefficients, dielectric constant, pyroelectric coefficient, etc. [19].

Many works are reported in literature on PZT thin films, but very few are reported on PZT fibres. The main problem of PZT fibres prepared by sol-gel process is its low strength. Shoko Yoshikawa et. al [20] reported a tensile strength of 36 to 40 MPa for specimens of 1 to 2 mm in length and 26 to 36 μm diameter. The strength reported in the earlier work in our lab [21] is 30-50 MPa. With this low strength it is very difficult to handle the fibres and use them in practical applications. The tensile strength value for bulk PZT ceramics is in the order of $\sim$76 MPa. Thus the fibre strength is low even in comparison with the bulk strength. Usually the fibres are much stronger than bulk. Thus the glass fibres can be easily made with strength exceeding 1 GPa. The reason for the low strength of the PZT fibres may be the occurence of defects during drying of gel or heat treatment of the fibres.

1.9 The Statement Of The Problem

The PZT fibres prepared by sol-gel process have strength which is an order of magnitude less than glass fibres or other commercially available ceramic fibres. The possible reason for the low strength is the presence of flaws which forms during or subsequent heat treatment of these fibres. Drying and firing steps are accompanied by removal of remaining organics and a large amount of shrinkage.

In the present work three different approaches to minimize the shrinkage and organic removal in the fibres will be explored. Firstly the effect of drying step will be studied by controlling the drying rate. Secondly the use of some chemicals called drying control chemical additives will be explored. Thirdly the sol will be partially converted to gel powder and this suspension of powder in the remaining sol will be gelled and fibres will be drawn from it.

Chapter 2

Experimental procedure

The process of preparing lead zirconate titanate (PZT) fibers and different characterization techniques used to study the fibres are described in this chapter. First the method of sol preparation is given in detail. The subsequent process of aging the sol, drawing the fibres from the gel, drying of fibres and their heat treatment is then described. The method of adding different additives used in the work is also mentioned. Then the characterization procedure used in the work, viz. thermogravimetric analysis (TGA), differential thermal analysis (DTA), X-ray diffraction (XRD), scanning electron microscopy (SEM) are given. At the end the method of strength measurement of the fibres by three-point bending method is described.

2.1   Procedure of preparing PZT fibres

PZT fibres are prepared by sol-gel process. The precursors used, method of preparing the sol and drawing of fibres from it are described in the following sections.

2.1.1   Precursors

The fibres are prepared using the sol-gel method. The different chemicals used in the work are given in Table 2.1. First the yield of metals as oxides from respective chemicals were determined.

To calculate the yield of PbO from lead acetate trihydrate (Pb-acetate), we have heated 1.50 gms of Pb-acetate in a platinum crucible at 600°C for 2 hours to form PbO powder. The formation of PbO was confirmed by X-ray diffraction. The yield of PbO

Table 2.1: Chemicals used in the present work

Compound	Formula	Molecular Weight	Density	Supplier
Zr(IV) Propoxide	$Zr(OC_3H_7)_4$	327.58	1.05	Fluka
Ti(IV) butoxide	$Ti(OC_4H_9)_4$	340.35	0.99	Alpha products
Pb-acetate	$Pb(CH_3CO_2)_2.3H_2O$	379.33	2.55	Aldrich
2-Methoxy ethanol	$CH_3OCH_2CH_2OH$	76.10	0.97	CDH
Formamide	$HCONH_2$	45.04	1.12	SD fine
Dimethyl Formamide	$HCON(CH_3)_2$	73.09	0.94	NICE
PEG-400	$H(OCH_2CH_2)_nOH$	380-420	1.11-1.14	Loba chem.
Nitric acid	HNO_3	63.01	1.4	NICE

was calculated using,

$$yield = \frac{(wt.of\,PbO\,formed)x(mol.wt.of\,Pb-acetate)}{(mol.wt\,of\,PbO)x[initial\,wt.of\,Pb-acetate(1.5gms)]}X100. \quad (2.1)$$

In our case 1.5 gm lead acetate gives 0.89 gms PbO. Thus the yield of PbO from Pb-acetate is 99.9%. Similarly the yield of ZrO_2 and TiO_2 from Zr(IV)-propoxide (Zrnp) and Ti(IV)-butoxide (Titb) were calculated. The yield from Zr(IV) propoxide was 74.88% and that from Ti(IV) butoxide was 100%.

The amounts of chemicals required to prepare PZT sol of composition which is $Pb_{1.10}(Zr_{0.53}Ti_{0.47})O_3$ were calculated considering the respective yield value as calculated above. We have added 10% extra lead to compensate the lead loss during heat treatment [22,23]. For example to prepare 0.01 M $Pb_{1.10}(Zr_{0.53}Ti_{0.47})O_3$ sol we have used 4.18 gm Pb-acetate, 2.34 gm Zr(IV) propoxide and 1.6 gm Ti(IV)butoxide. 6 gm of 2-Methoxy ethanol was used to dissolve Pb-acetate. The same amount of 2-Methoxy ethanol was used to dissolve both Zrnp and Titb. 0.1 gm Nitric acid with 3 gm 2-Methoxy ethanol was used as catalyst. Detailed processing of PZT sol-gel precursors for fiber formation has been reported by Selvraj et al. [24]. The general principle of the reactions of the precursors has been reported by Guglielmi et al. [25].

2.1.2 Sol Preparation

The PZT sol was prepared following broadly the procedures adopted earlier in our laboratory [21]. The apparatus used to prepare the sol is shown in fig. 2.1. First Pb acetate was dissolved in 2-Methoxy ethanol in a three neck flask assembly with
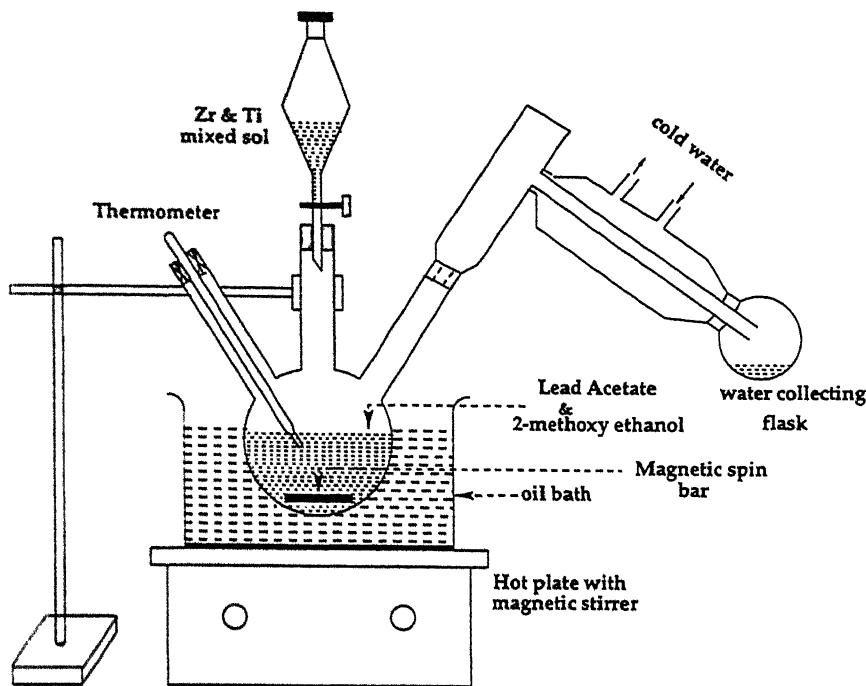
Figure 2.1: Apparatus for sol preparation

a condenser. Then it was heated to 135°C and kept at that temperature for about 20 minutes to remove all the water of crystallization. This was necessary because the alkoxides readily react with water to form particles . Zrnp and Titb were mixed seperately in a glove box in which the humidity was kept below 15%. The mixture was stirred for 5 minutes and 2-Methoxy ethanol was added dropwise into it. This solution was stirred in the glove box for 30 minutes. This sol was then added dropwise to the lead acetate solution in the three neck flask, maintaining the temperature at 120°C. The entire solution was stirred slowly in the flask at 120°C for 30 minutes. It was then cooled to room temperature, and nitric acid with 2-Methoxy ethanol was added to it. The solution was stirred for 5 minutes. The sol thus prepared has a golden yellow colour.

We have tried to use different amounts of water with the sol to form particles. After preparing the sol, water was added to it gradually with the help of a dropper at room temperature. Stirring was done continuously. Then the resulting sol was gelled in an oven. We have been successful in drawing fibres with 2 mole and 4 mole of water per mole of alkoxide by this process.

2.1.3   Aging of sol and addition of DCCA:

The sol was kept in a 100 ml beaker covered with aluminium foil. It was kept in an oven at 120°C. Solvent gradually evaporates and gelation takes place. The rate of evaporation depends upon temperature, surface area of evaporating body and whether the system is open or closed. so these parameters besides the rheological properties of the sol can be controlled to vary the gelation time. In our case the sol becomes spinnable i.e fibres could be drawn from it, after aging for about 9 to 14 hours. The sol gradually changes from golden yellow to dark red in colour and gradually becomes viscous.

The chemical additives used in the work i.e, formamide, dimethyl formamide, PEG-400 were added during the aging process [27]. It was observed that. adding this chemicals at the begening does not make the sol spinnable. We have added the additives after aging for about 8 to 9 hours, at the time when the sol just becomes spinnable. Then it was further aged in oven for about 1 hour. Large shrinkage of sol occurs (it becomes ~1/6) when it becomes spinnable at the end of aging.

2.1.4   Drawing of fibres and Drying them:

Fibres from the gel was drawn using a pointed glass rod. The pointed portion of the rod was dipped in the gel and gradually drawn out from it by hand at almost a constant speed. We have drawn fibres from PZT gel and PZT with formamide (1:1/2; 1:1/4; 1:1/8 molar ratio) PZT with DMF (1:1/2; 1:1/4; 1:1/8 molar ratio) and PZT with PEG-400 (1:0.05; 1:0.1 molar ratio). Fibres of dia. from 10 to $100 \mu m$ and length upto 60 cm were drawn by this method. The gel when it stops giving fibres can be reused by diluting with ~5 ml of 2-Methoxy ethanol and aging further for about 10 minutes.

The fibres with chemical additives were dried at room temperature for approximately 24 hours. Fibres without any additives were slow dried in vapours of 2-Methoxy ethanol for 3 days, 7 days and 20 days. For slow drying method a petri dish of 15 cm ϕ was covered tightly with aluminium foil. Pin holes were made all round the foil at a spacing of about 0.5 cm and 10 ml of 2-Methoxy ethanol was kept inside it in a small glass dish. After 24 hours fibres were drawn and were cut in length of about 10 cm and placed inside the dish. This arrangement was kept for 3 days, 7 days, and 20 days after which fibres were taken out from it.

2.1.5 Heat treatment of fibres

The as prepared fibres contain substantial amount of organics. These get removed during heat treatment and excessive shrinkage occurs during it. This may introduce cracks and flaws in the fibres resulting in low strength. For this a proper heat treatment shedule is to be found out. We have performed thermal analysis i.e, Differential Thermal Analysis (DTA) and Thermo-gravimetric Analysis (TGA) described later, to identify the physico-chemical changes that occur during the heat treatment. The heat treatment shedule is shown in Fig 3.6.

2.2 Characterization of gels and fibres

2.2.1 Thermogravimetric Analysis (TGA)

The gel from which fibres were drawn is ground in a mortar pestle to form fine powder. A small amount of powder (about 100 mg) (W_1) is taken in an alumina crucible which is hung from an electronic balance (ER-100A, Afcoset, India) by a platinum wire into an electrically heated vertical furnace. The sample is heated at a constant rate of 2^oC/min. The weight of sample (W_2) is recorded as a function of temperature, from room temperature to 800^oC. The weight percent of sample, $\frac{W_1-W_2}{W_1}X100$ vs. temperature(T) gives the TGA plot. Some errors in the experiment may occur at higher temperature due to buoyancy.

2.2.2 Differential Thermal Analysis (DTA)

A DTA apparatus (DTA 50, Shimadzu, Japan) with alumina powder as inert reference was used. The gel derived crushed fine powder was heated at 10^oC/min in a platinum crucible and air ambient to yield the DTA plot.

2.2.3 Optical Microscopy

After drying, the fibres were examined in an optical microscope (Carl zeiss, Germany) under reflected light at X100. The surface smoothness and gradually tapered cross section of the fibres were observed at this magnification.

Table 2.2: Operating Parameters of XRD

Accelerating Voltage	30KV
Scanning Speed(SS)	1.2^o/min.
Chart Speed(CS)	12mm./min.
Counts per minute(CPM)	10
Time Constant(TC)	10sec.

2.2.4 X-ray diffraction

The phase analysis is carried out for the crushed, sintered fibres by x-ray diffraction method, using an x-ray diffractometer (Rich seifert ISO-Debyflex 2020, Germany). CuK_α radition ($\lambda = 1.5405$ Å) is used with a Ni monochromator. The powder samples are spread evenly on the surface of a glass slide with the addition of a few drops of acetone, so that the powder sticks to the glass slide.

The X-ray diffraction plots (intensity Vs. 2θ) are recorded in a 2θ range from 20° to 70°. The operating conditions are given in Table 2.2.

The interplaner spacing d is calculated using Bragg's law:

$$n\lambda = 2dsin(\theta) \tag{2.2}$$

where,

n = order of diffraction,

λ = X-ray wavelength,

θ = Bragg's angle.

2.2.5 Scanning Electron Microscopy:

The cross-section of the fibres are studied by a scanning electron microscope (JSM, 840A, JEOL, JAPAN). The as-prepared as well as the sintered fibres were cut to length of about 3 - 4 mm. They were then fixed vertically on top of a 1 cm. cylindrical brass stub, using silver paste. A thin Au layer is then deposited on the fibres by a dc sputter coating unit (Hummer VIA, Anatech Ltd. U.S.A.). They are then observed under SEM to study the presence of flaws and grain formation.
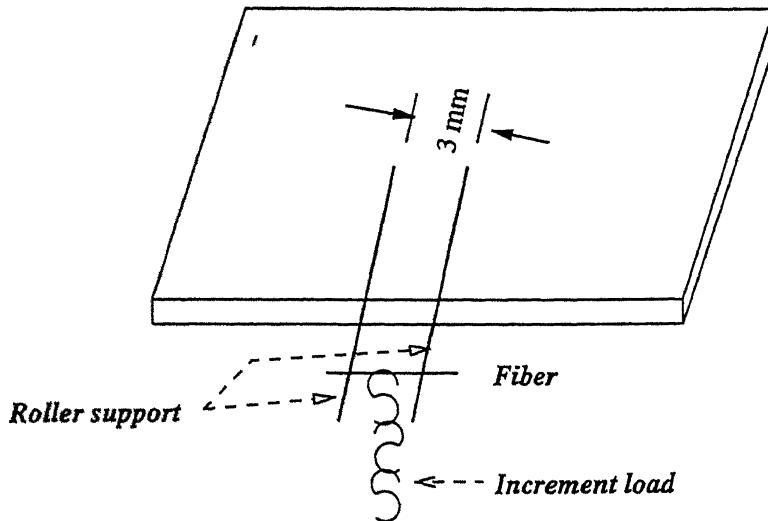
Figure 2.2: Strength measurement by three-point bending method

2.3   Measurement of Strength of Fibres

A standard tensile testing machine cannot be used to measure the strength of PZT fibres because of their low strength. We have used a method of three point bending to calculate the strength of the fibres. The apparatus is shown in Fig 2.2. Two metal cylinders of 0.8 mm diameter are fixed on a stand with a span length of 3 mm. Fibres are cut in length slightly greater than 3 mm. They are then placed lightly on the two cylinders with small quantity of some adhesives.

Incremental loads in the order of 0.005 to 0.01 gm were then applied very lightly on the middle of the fibres. The failure load is determined by weighing all the incremental loads together, when the fibre breaks. The cross-sectional diameter of the fibre at the point of rupture is measured using an optical microscope and a shadowgraphe. The strength of the fibres are then calculated using the relation,

$$\sigma = \frac{8}{\pi} X \frac{PL}{d^3}. \tag{2.3}$$

Where P is the failure load, L is the span length (3 mm) and d is the diameter of the fibre at the point of failure.

To correct the different errors in the experiment, a factor of 0.05 was determined in our lab by measuring the strength of glass fibres by this method and also by a standard tensile testing machine [INSTRON 1190] [18]. The strength value obtained by three point bending method are multiplied by 0.05 to obtain the actual strength.

2.3.1   Analysis of the strength data

The strength data was analysed using the three parameter Weibull distribution given by,

$$P(\sigma) = 1 - exp[-\frac{S}{S_o}(\frac{\sigma}{\sigma_o})^m]$$

(2.4)

and,

$$P(\sigma) = 1 - exp[-\frac{V}{V_o}(\frac{\sigma}{\sigma_o})^m]$$

(2.5)

Where,

$P(\sigma)$ is the probability that the strength of the fibres $\leq \sigma$, d is the diameter of the fibres, m is the weibull modulus, σ_o is the normalised strength, d_o is the normalised diameter chosen to be 10 μm. S, S_o, represents surface area and V, V_o represents volume.

The above two equation reduces to

$$\ln[-\ln(1 - P(\sigma)] - \ln(\frac{d}{10}) = m \ln \sigma - m \ln \sigma_o$$

(2.6)

for surface, and

$$\ln[-\ln(1 - P(\sigma)] - 2\ln(\frac{d}{10}) = m \ln \sigma - m \ln \sigma_o$$

(2.7)

for volume. These equations are in the straight line form Y = m.X + C.

The Weibull plot is determined by taking

$$X = \ln(\sigma);$$

(2.8)

$$Y = \ln[-\ln(1 - P(\sigma)] - \ln(\frac{d}{10}) \; for \; surface$$

(2.9)

and,

$$Y = \ln[-\ln(1 - P(\sigma)] - 2\ln(\frac{d}{10}) \; for \; volume$$

(2.10)

The best fitted straight line is drawn in the plot by maximizing the correlation coefficient. The sum of squares was used as a measure of fit between the distribution function and the data[28,29]. The value of slope of the straight line (m) and Y intercept

(C) is determined. Then the standardized strength for 10 μm fibres are calculated by using the relation,

$$\sigma_o = exp(-c/m) \qquad (2.11)$$

By comparing the σ_o values and their correlation coefficient, the nature of defects causing low strength can be understood.

Chapter 3

Results and Discussion

3.1   Thermogravimetric Analysis

The TGA plot is shown in figure 3.1 and is plotted by taking percentage weight loss with respect to the initial weight, vs. temperature. It is found that the total weight loss for gel with formamide and dimethylformamide is more than that with PZT gel without any additives. This is due to the additional removal of additives along with the organics in the gel with formamide and dimethylformamide additives. The initial slope in the plot (upto 150°C) is very steep in case of gel with additives. This is due to the removal of solvents remaining in the gel. In case of PZT gel it seems solvent has already escaped from the gel before the TGA experiment. The second slope in the plot between 200 and 300(°C) for all the cases is almost same and represents the removal of organics coming from the alkoxide precursor for gel preparation. From 320°C to 480°C all the plots tend to be parallel to the temperature axis, showing no weight loss. From about 480°C to 650°C a slow change in slope is noted for all the cases. Some organics with higher molecular weight get removed at this temperature range. After 700°C all the plot are flat indicating that all the organics/additives have been removed.

3.2   Differential Thermal Analysis

The DTA plots for PZT gel powder, PZT with formamide and PZT with DMF are shown in figures 3.2, 3.3 and 3.4 respectively. The first endothermic peak between 75°C to 100°C in all the cases is due to the removal of water and alcohol from the gel. The endothermic peak present at ~248°C for PZT-Formamide gel represents the dissociation of lead acetate. The exothermic peak present at around 310°C in all the
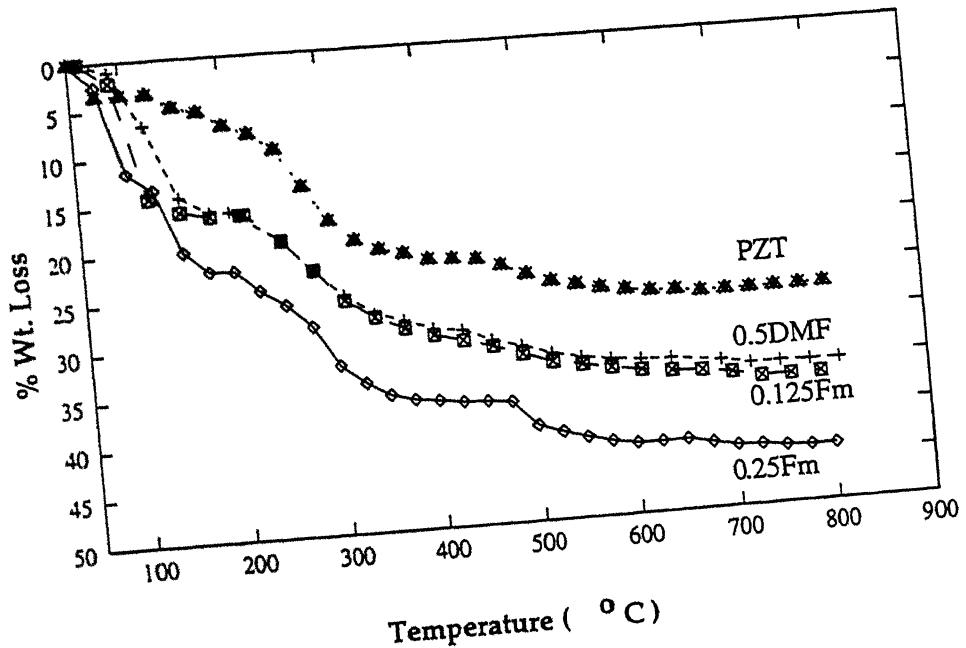
Figure 3.1: TGA Plot

case indicates the crystallization of PbO. The exothermic peaks present after 550°C represents crystallization.

Figure 3.5 represents the DTA plot of PZT gel with PEG-400 additives taken after 3 months. There is only one sharp peak at 321.24°C. This seems to be due to the crystallization of PbO. Further crystallization is not found upto 1000°C for this case.

3.3 Heat Treatment of Fibres

Based on the DTA and TGA results we designed the heat treatment shedule (shown in figure 3.6) for the gel derived fibres. At 300°C the hold time is 12 hours to ensure complete removal of organics and solvents that occurs upto this temperature. At 600°C we hold further for 2 hours for the removal of higher molecular weight organics. The heating rate upto 600°C is 1°C/min. Higher heating rate result in breakage of the fibres to very small pieces. This is due to the higher rate of removal of organics from the fibres. Also higher heating rates may result in black fibres due to the formation of carbon thus indicating improper oxidation of organics. From 600°C to 1000°C we heat at 3°C/min to minimize lead loss which occurs at this range of temperature. At 1000°C we hold for 10 minutes for proper crystallization after which we cool to room temperature at 3°C/min. This heating shedule yields fibres with minimum breakage.

29
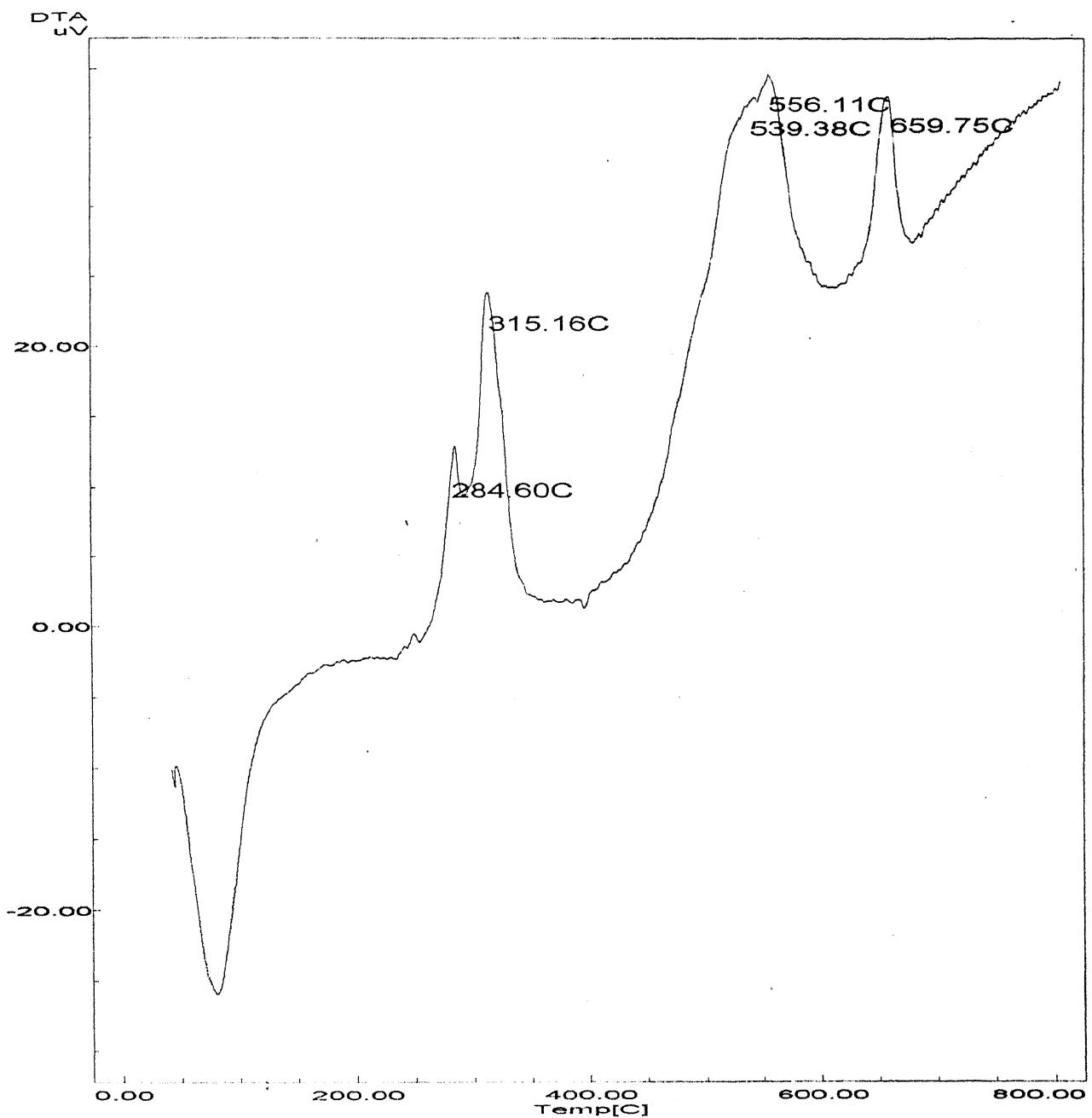
Figure 3.2: DTA of PZT gel powder.
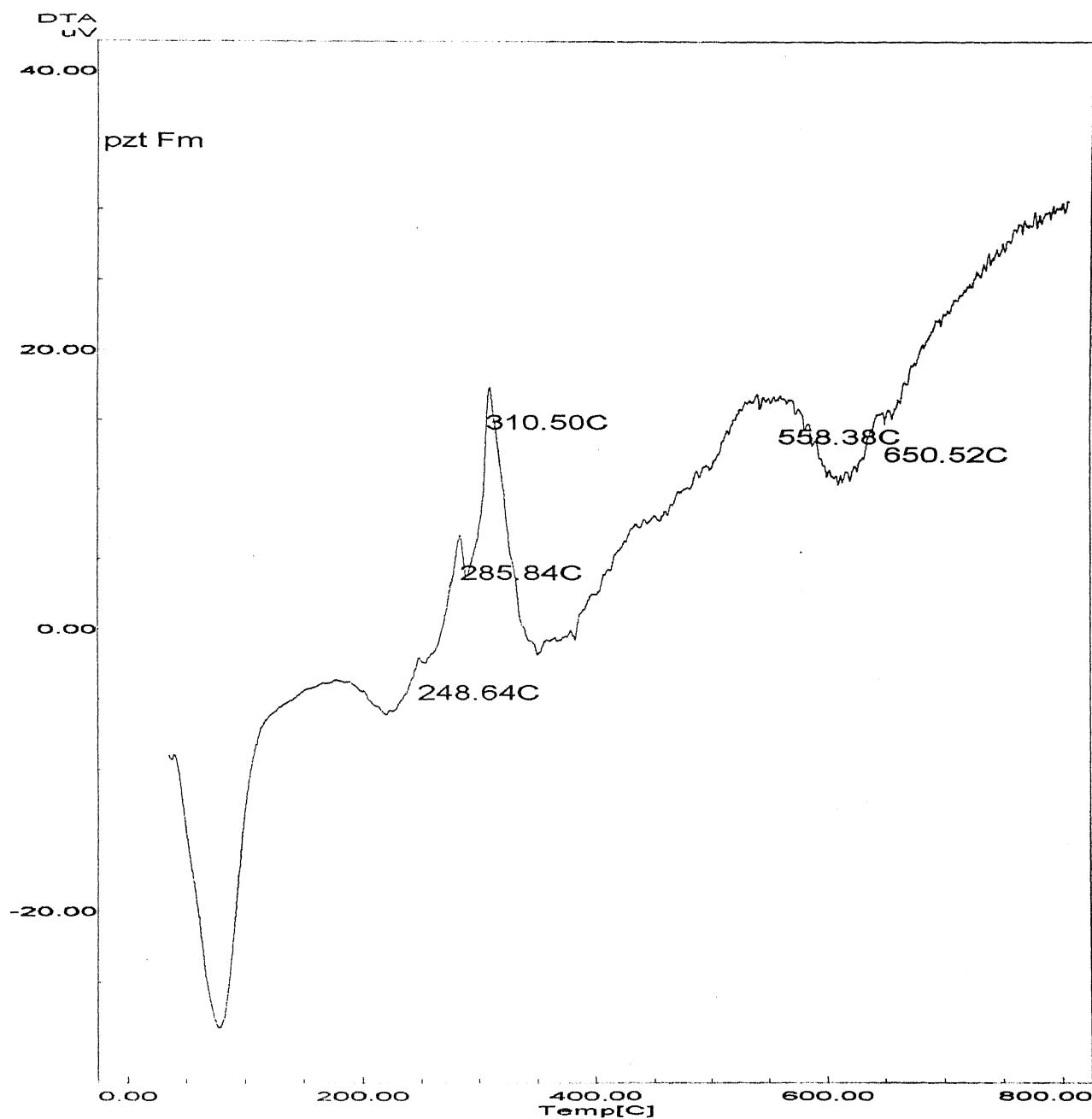
Figure 3.3: DTA of PZT-Fm (1:0.25) gel powder.
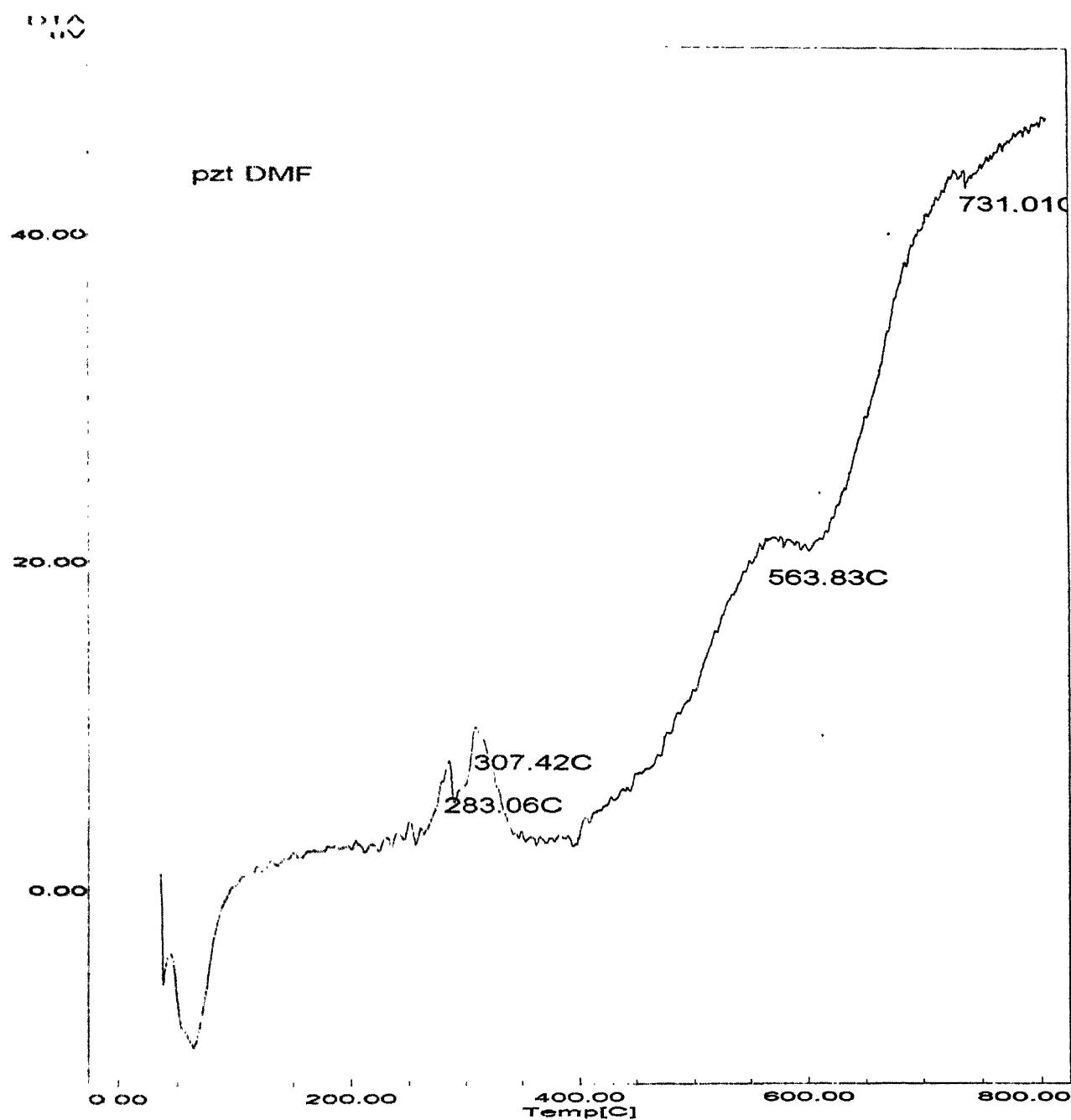
Figure 3.4: DTA of PZT-DMF (1:0.25) gel powder.

315.40C
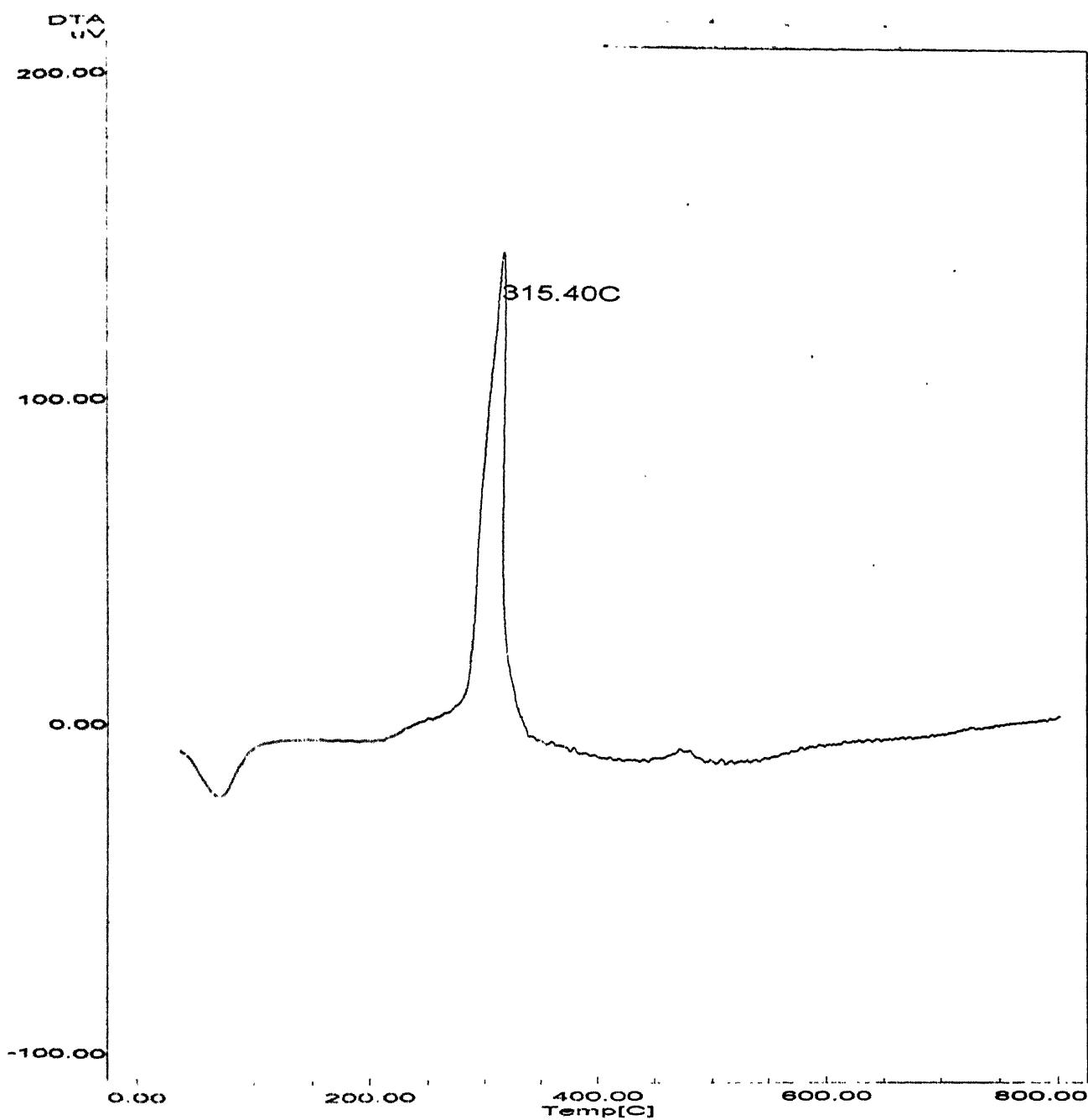
Figure 3.5: DTA of PZT-PEG-400(1:0.1) gel powder.

Figure 3.6: Heat Treatment Shedule

The lead loss as indicated in chapter 2 can be understood from the colour of the fibres after heat treatment. Fibres from which substantial lead is lost become lighter in comparison with the fibres with little lead loss which are reddish in colour. It is found that fibres with smaller diameter (less than 40 μm) are fainter in colour and more flexible in comparison with larger diameter fibres which seems to be more brittle.

3.4 X-Ray Diffraction

XRD spectra of all the fibres heat treated at 1000°C revealed the presence of well crystallized pervoskite phase (figure 3.7). The results are summerised in table 3.1.

3.5 Microstructure Observations

Figure 3.6 shows the micrographs of as prepared fibres with 2 and 4 moles of water. Cracks in the cross section seems to be increased with the amount of water added to the sol. Figure 3.8 shows the cross-sectional view of normal dried fibres. and fibres slow dried in vapours of 2-methoxy ethanol for 3 days and 7 days respectively. Cracks

Figure 3.7: X-ray diffractrograms of PZT fibres and fibres made with different additives.

Table 3.1: X-ray diffraction results from fibres prepared using 1:0.25 formamide

Sl. No.	2θ (degree)	(hkl)	d ($\overset{\circ}{A}$)
1	22	(100)	4.04
2	31.3	(110)	2.85
3	38.3	(111)	2.35
4	44.5	(200)	2.02
5	50.2	(210)	1.81
6	55.4	(211)	1.66
7	64.5	(022)	1.45

are observed in the cross section of the normal dried fibres. Extensive cracking is found in the 3 day dried sample but no cracks are present in the cross-sections of the 7 day dried fibres.Figure 3.9 shows the microstructure of fibres prepared with different amounts of chemical additives. We observed no cracking in the cross-section with DMF and formamide additives but with PEG, cracks in the fibres are visible.

The high magnification cross-sectional views of the as drawn fibres are shown in figure 3.10. It is found that very fine scale uniformly distributed porosity is present in case of formamide.

Fibres prepared with PEG-400 and sintered at $1000^{\circ}C$ are shown in figure 3.11. There are no cracks present in the cross-section. We have observed cracks in the same fibres in the as drawn state. Those cracks seem to have healed producing a dense microstructure. We have noted the highest strength with these fibres as reported later.

Figure 3.13 shows the cross-sectional view of sintered fibres with different amounts of DCCA added. Figure 3.14 gives the cross-section of 7 day slow dried and 20 day slow dried fibres. We have noted that cracks have re-appeared with 7 day fibres but with 20 days of slow drying they were not observed. We found an increase in strength with the time of slow drying as reported later.

figure 3.15 represents the high magnification cross-sectional views of fibres prepared with different additives. Figure 3.16 shows the high magnification cross-sectional views of 7 days and 20 days slow dried fibres. 7 days slow dried fibres seems to have larger grains than 20 day slow dried fibres. The finer grain size observed in 20 day slow dried fibres is probably the cause of the higher strength obtained in it as reported later.

(a)

(b)

Figure 3.8: SEM micrographs of the cross-section of as prepared fibres with (a) 2 moles of water (b) 4 moles of water

[Cracks are observed in both the cases]

(a)
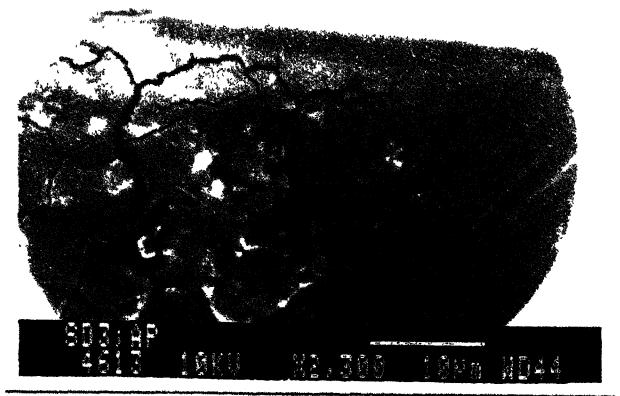
(b)
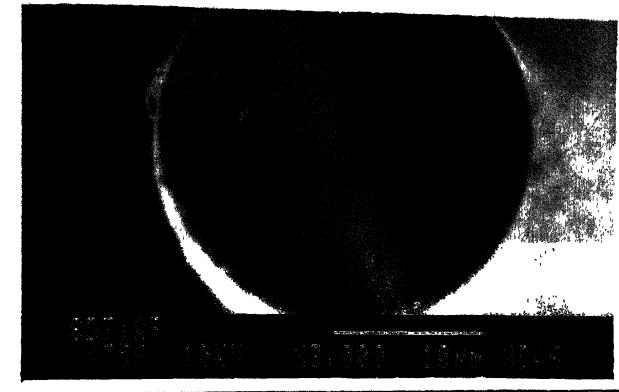
(c)

Figure 3.9: SEM micrographs of the cross-section of as prepared fibres (a)Normal dried
(b) Dried 3 days (c) Dried 7 days
[Extensive cracking in 3 day sample but no cracking in 7 day sample]
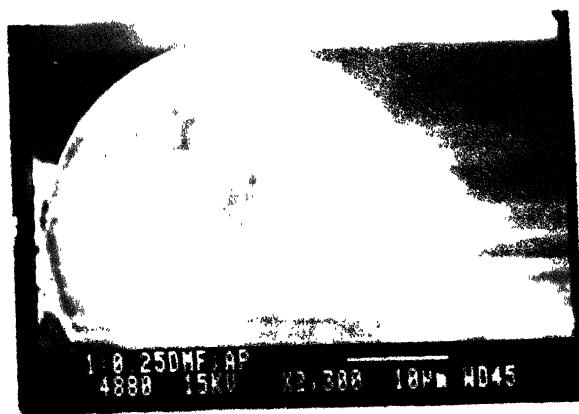
(a)
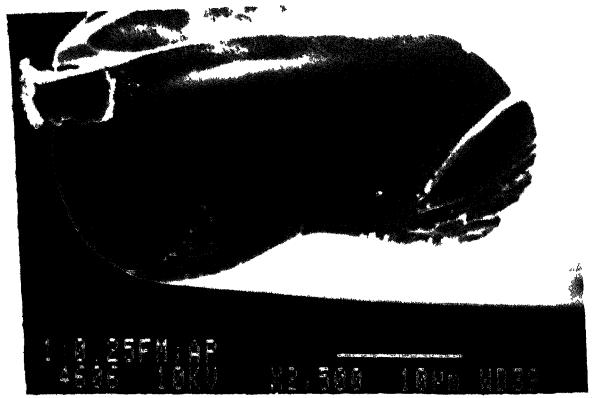
(b)

(c)

Figure 3.10: SEM micrographs of the cross-section of as prepared fibres with (a) 0.25 mole DMF (b)0.25 mole Formamide (c) 0.1 mole PEG-400

[Cracks are controlled by DMF and Formamide addition but with PEG there are cracks in the cross-section]

(a)

(b)

(c)
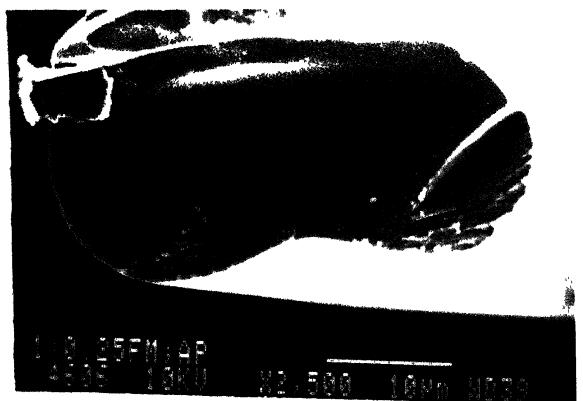
Figure 3.10: SEM micrographs of the cross-section of as prepared fibres with (a) 0.25 mole DMF (b)0.25 mole Formamide (c) 0.1 mole PEG-400

[Cracks are controlled by DMF and Formamide addition but with PEG there are cracks in the cross-section]

(a)
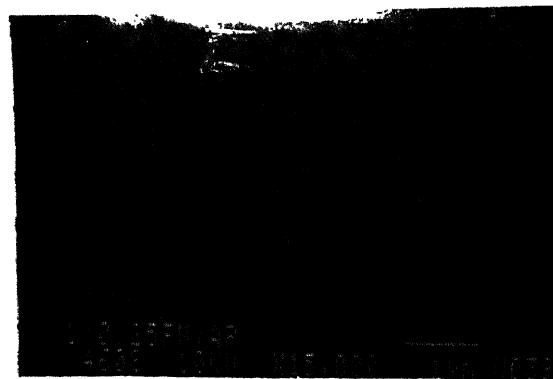
(b)
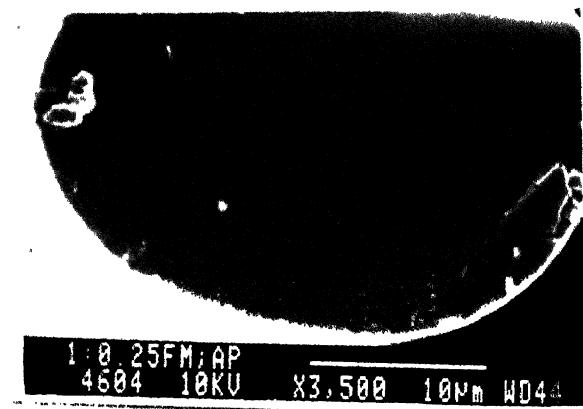
(c)

Figure 3.11: High magnification cross-sectional views of as prepared fibres prepared using different DCCA's. (a) with 0.25 mole DMF (b) with 0.25 mole Formamide (c) same as (b) but of lower magnification

[Very fine scale uniformly distributed porosity is present in case of formamide]

(a)

(b)

Figure 3.12: SEM micrographs of the cross-section of sintered fibres with (a) 0.05 mole PEG-400 (b)0.1 mole PEG-400
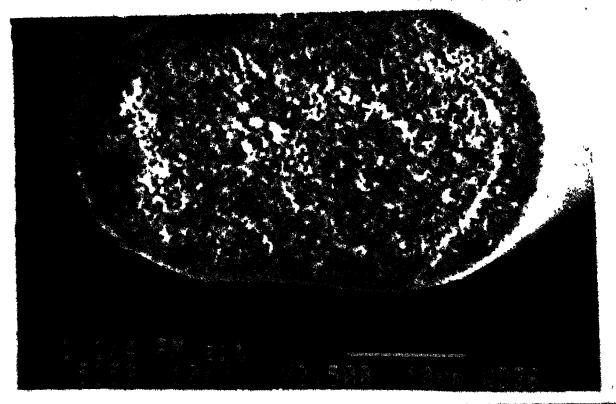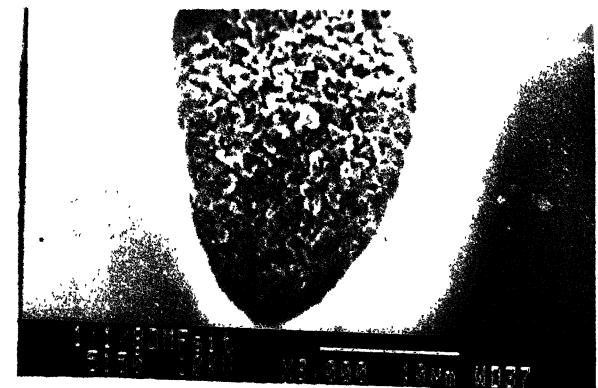
(a)   (b)
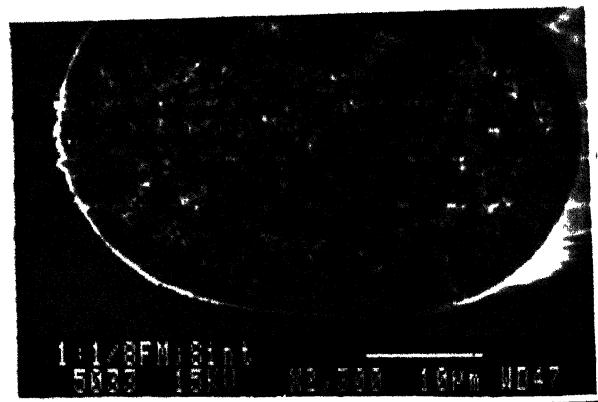
(c)

Figure 3.13: SEM micrographs of the cross-section of sintered fibres with (a) 0.25 mole Formamide (b)0.125 mole DMF (c) 0.125 mole Formamide

(a)
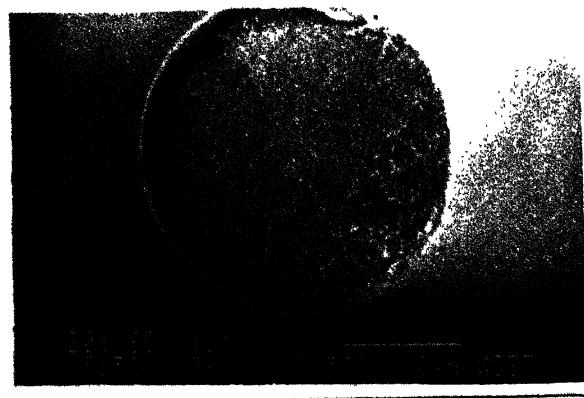
(b)

Figure 3.14: SEM micrographs of the cross-section of sintered fibres (a) 7 day slow dried (b)20 day slow dried

[cracks re-appearing with 7 day slow drying]

(a)

(b)
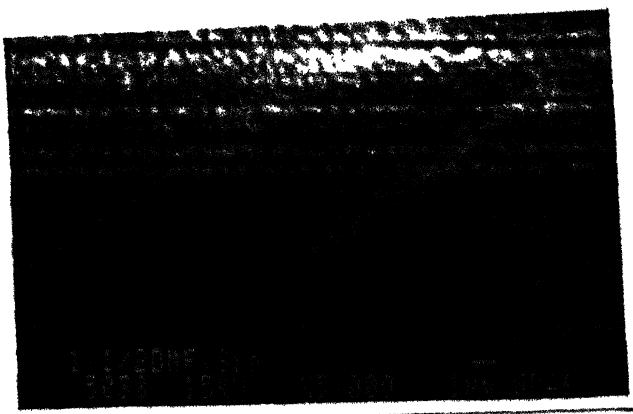
(c)
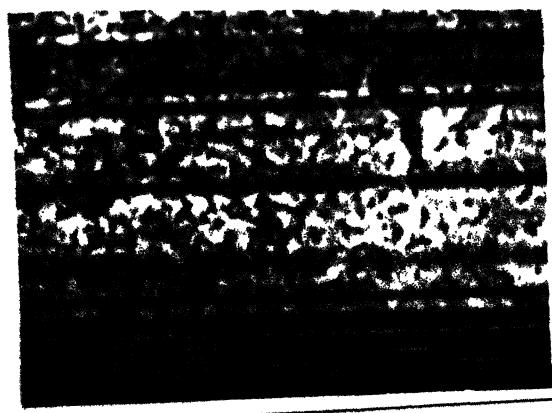
(d)

Figure 3.15: High magnification cross-sectional views of sintered fibres prepared using different DCCA's. (a) with 0.25 mole DMF (b) with 0.125 mole DMF (c) with 0.5 mole DMF (d) with 0.1 mole PEG-400

(a)
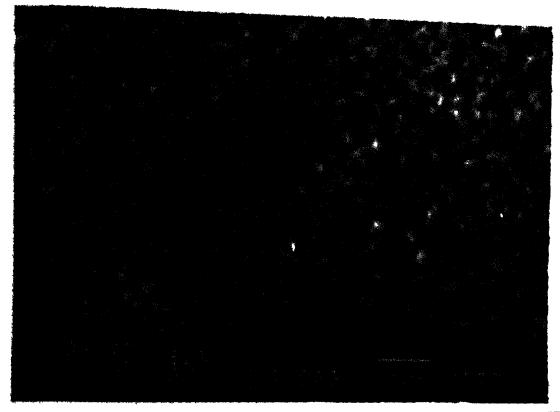
(b)

Figure 3.16: High magnification cross-sectional views of sintered fibres (a) 7 day slow dried (b) 20 day slow dried

45

3.6 Strength of Fibres

The strength of the PZT fibres was measured by three point bending method described in chapter 2. The as prepared fibres were too fragile to be used for strength measurements. Only a few measurements, not enough for analysis could be obtained on the as prepared fibres except those prepared using PEG. For the PEG fibres, which were most fragile in the as prepared state, no strength measurement at all could be done. The plots of strength vs. diameter for sintered fibres are shown in figure 3.17 to 3.28. The Weibull plot for two cases (with volume and surface normalization for each case) are shown in figure 3.29 to 3.32. The Weibull parameter m and σ_o for sintered fibres assuming surface flaws and volume flaws are listed in table 3.2. Also it is noted from the table that better correlation is obtained by considering the flaws to be on the surface. Thus the strength of the fibres is determined by surface flaws.

The slow dried fibres show an increase in strength with longer time of drying. Thus slow dried 20 days sintered fibres (SD20) have a σ_{o_s} value of 46.5 MPa in comparison with slow dried 7 (SD7) days fiber with $\sigma_{o_s} = 31.9$ MPa.

Fibres with dimethylformamide (DMF) shows an increased strength than the fibres with formamide. The strength obtained in fibres prepared with PEG-400 is highest. With 0.05 mole of PEG-400 the strength is 92.80 MPa. The remarkable observation is that the PEG fibres show cracks in the as prepared condition which heal after sintering and give a high strength.
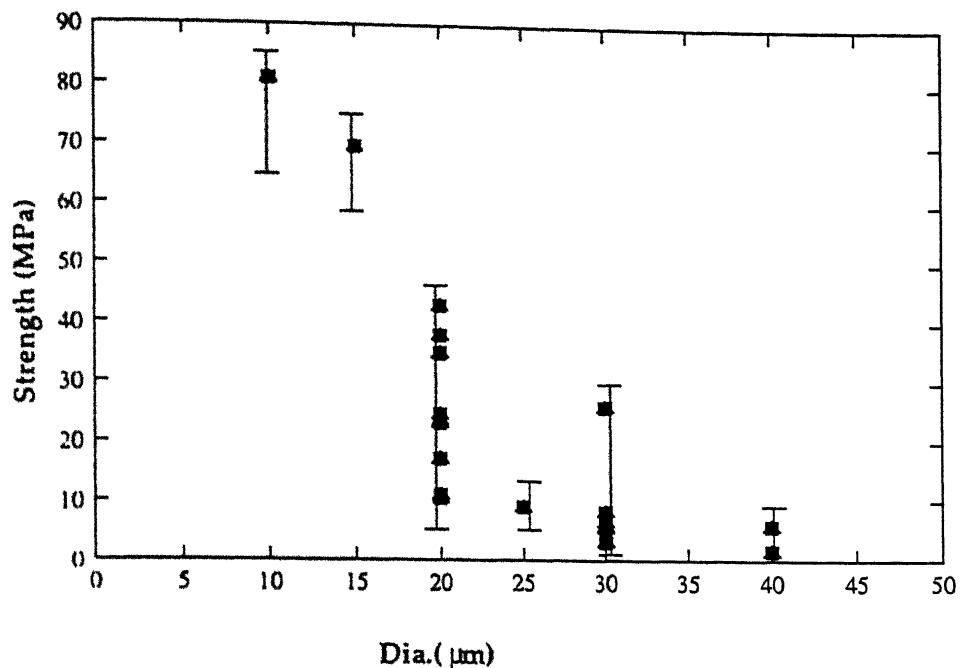
Figure 3.17: Strength vs Dia: PZT fibres with 0.125 mole Fm
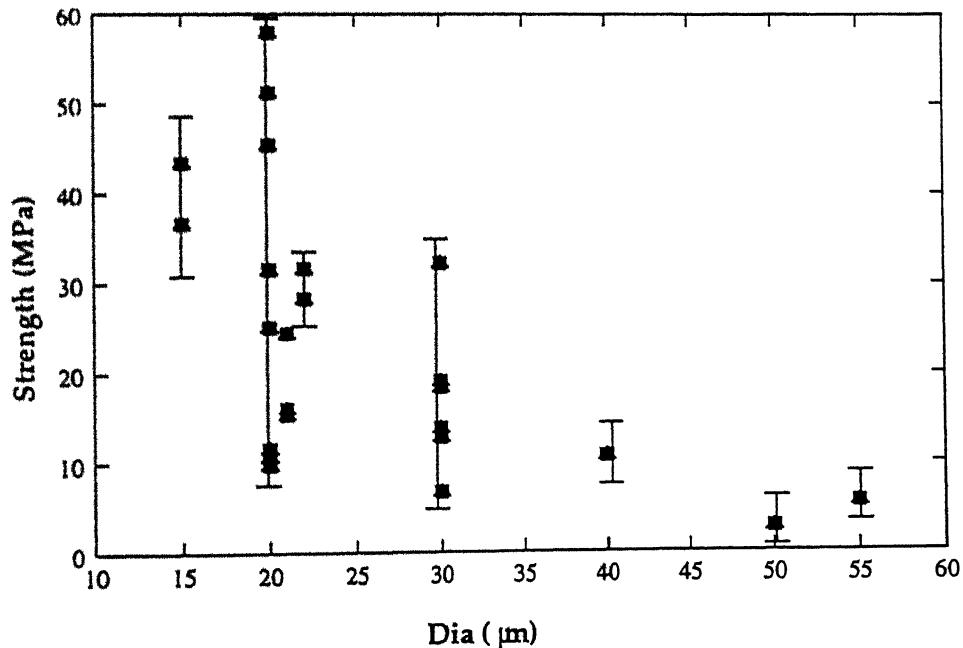


Figure 3.18: Strength vs Dia:PZT fibres with 0.25 mole Fm
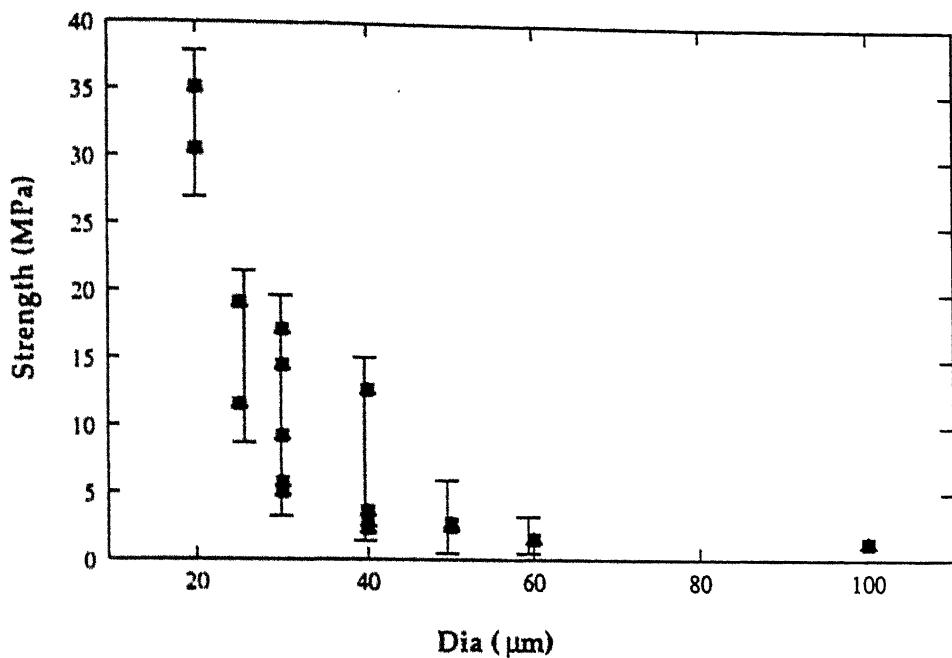
Figure 3.19: Strength vs Dia: PZT fibres with 0.5 mole Fm
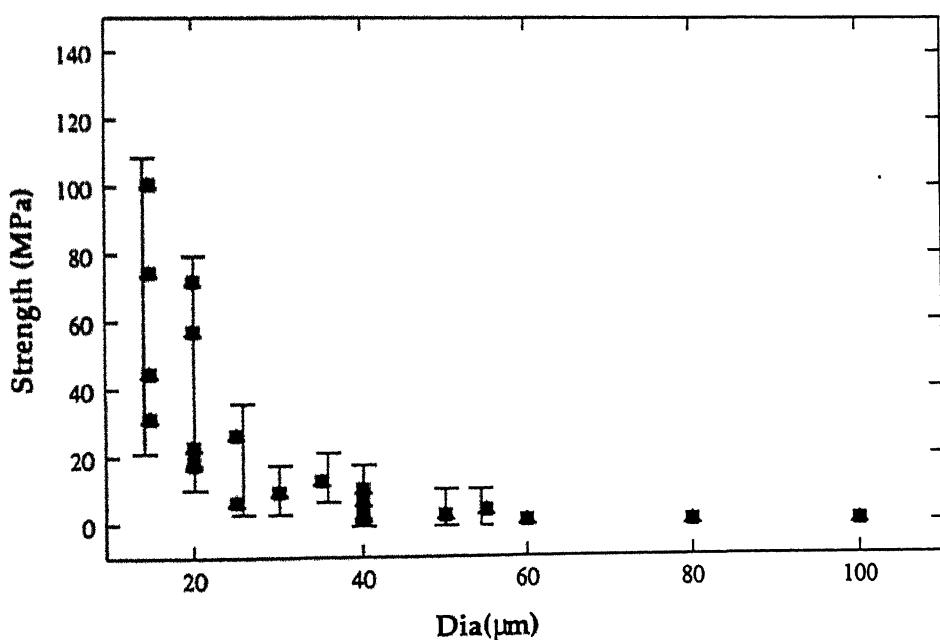
Figure 3.20: Strength vs Dia: PZT fibres with 0.125 mole DMF

48
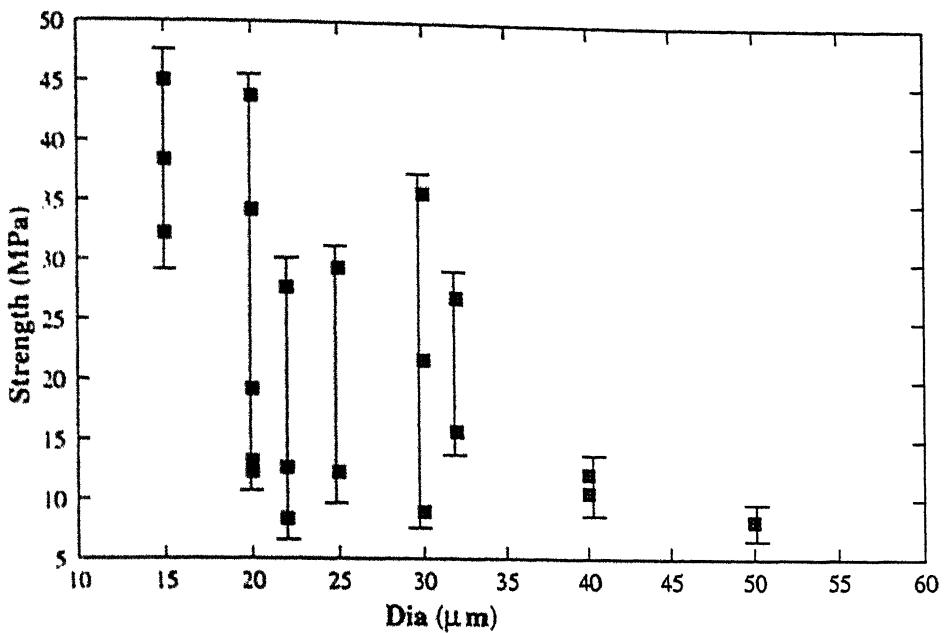
Figure 3.21: Strength vs Dia: PZT fibres with 0.25 mole DMF
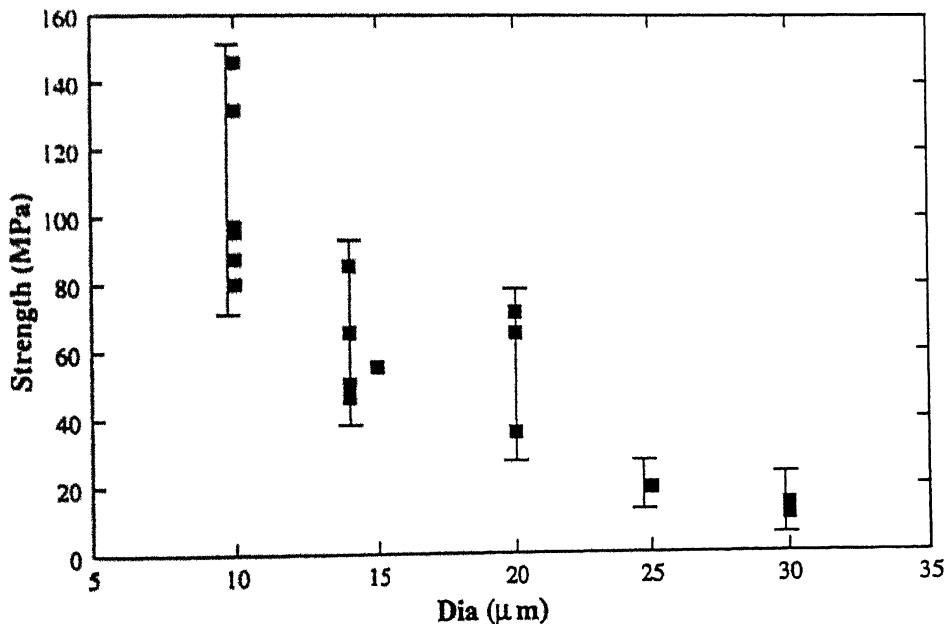
Figure 3.22: Strength vs Dia: PZT fibres with 0.5 mole DMF

49
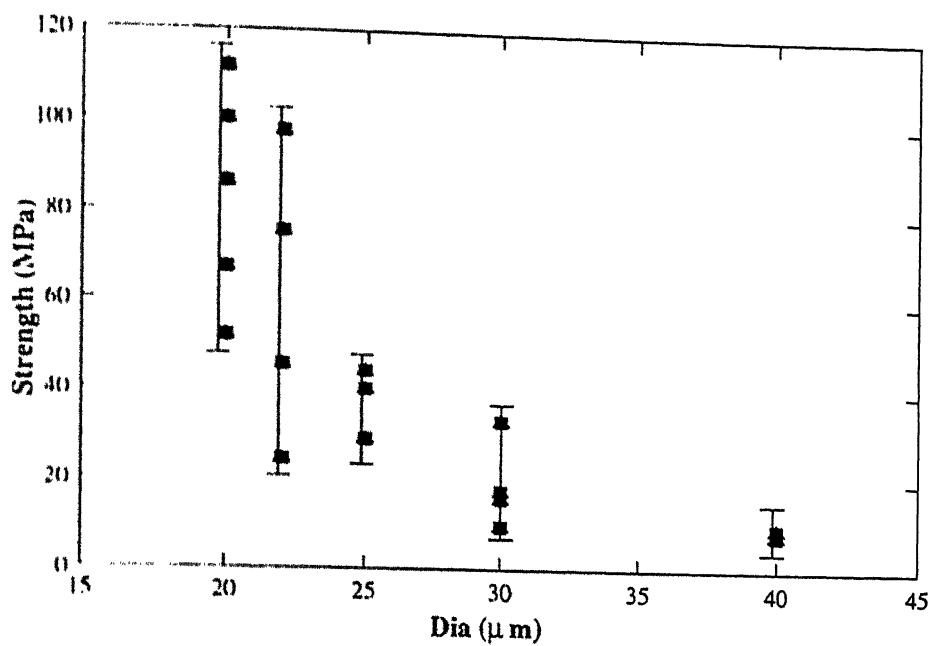
Figure 3.23: Strength vs Dia: PZT fibres with 0.05 mole PEG
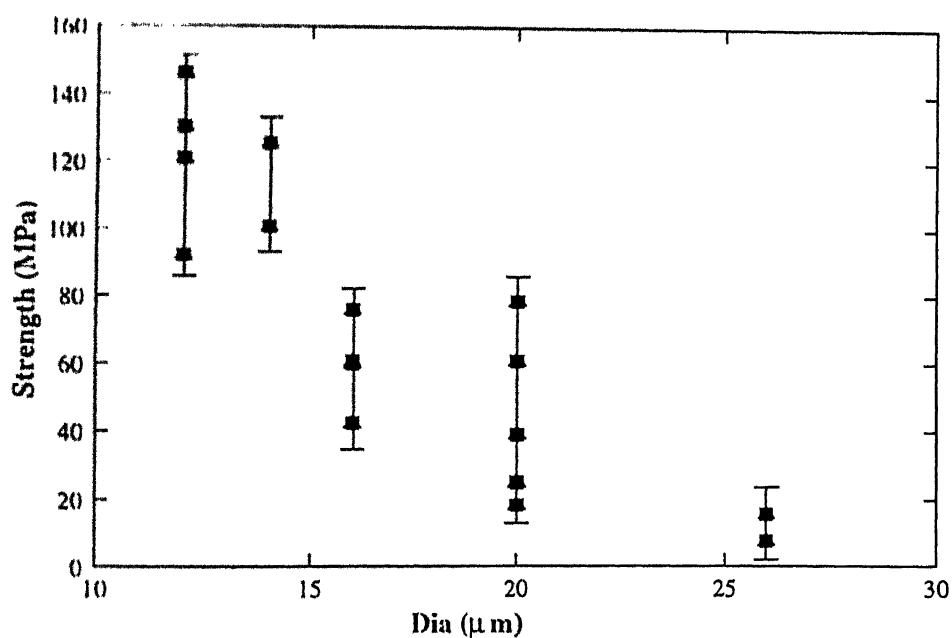
Figure 3.24: Strength vs Dia: PZT fibres with 0.1 mole PEG
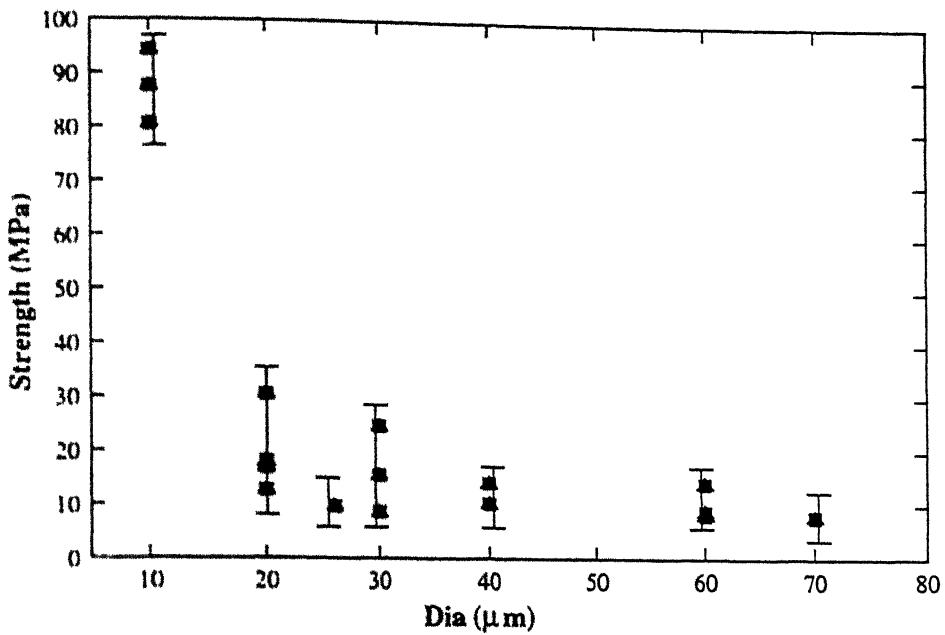
Figure 3.25: Strength vs Dia: PZT fibres with SD7
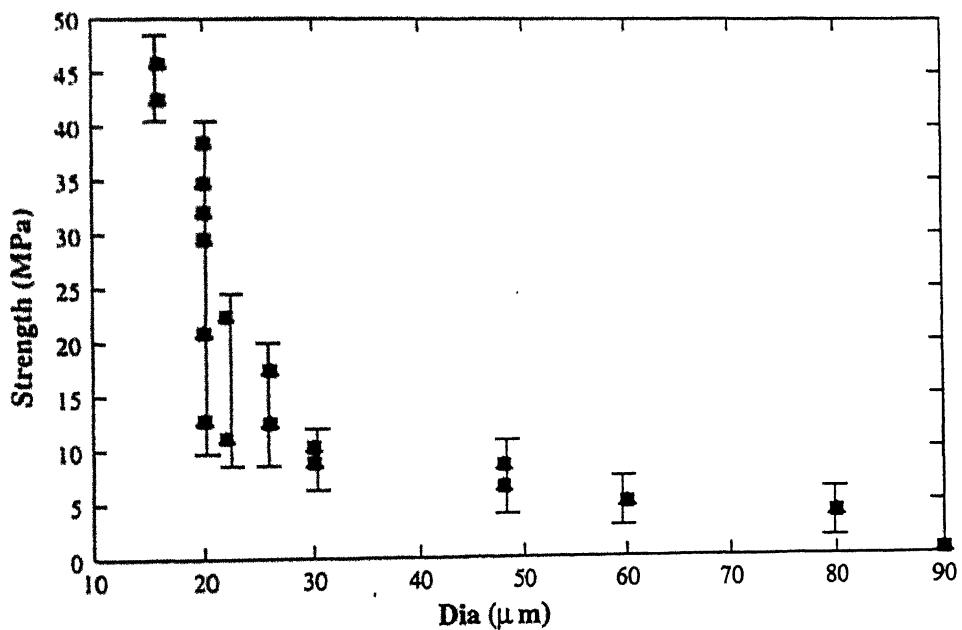
Figure 3.26: Strength vs Dia: PZT fibres with SD20

51
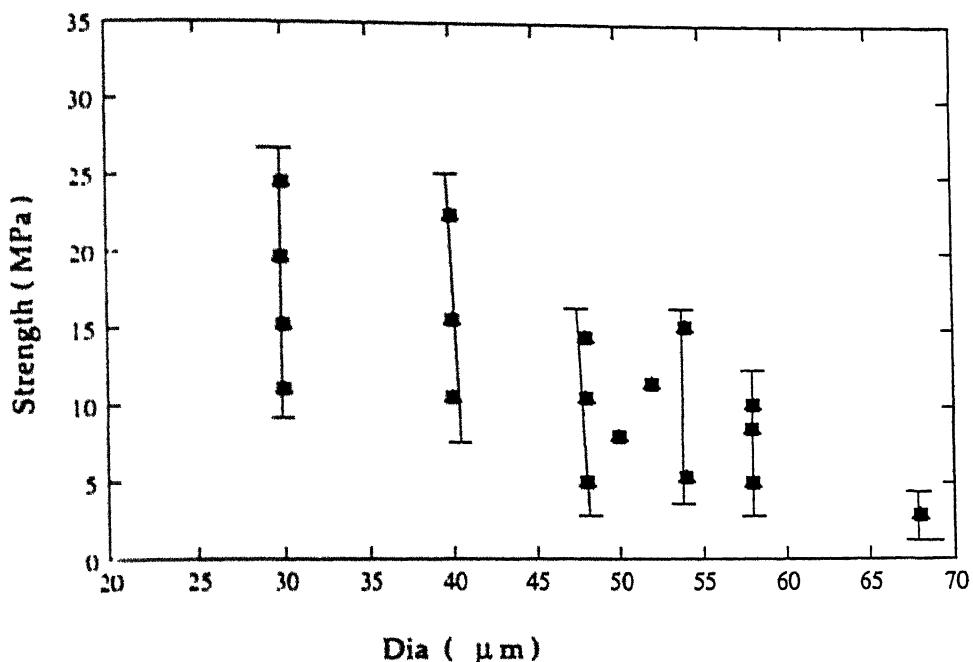
Figure 3.27: Strength vs Dia: PZT fibres with 2m water
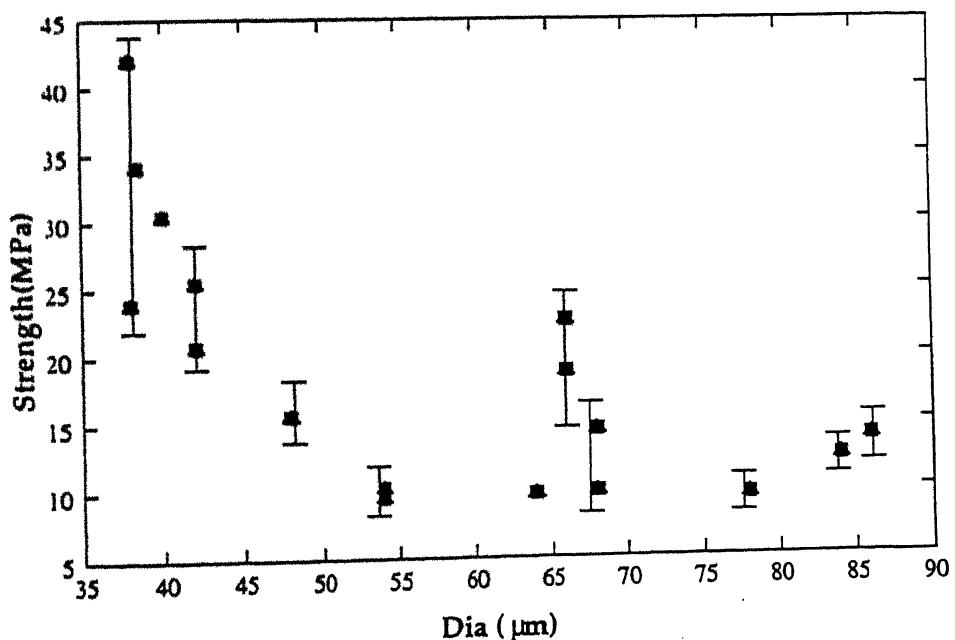
Figure 3.28: Strength vs Dia: PZT fibres with 4m water
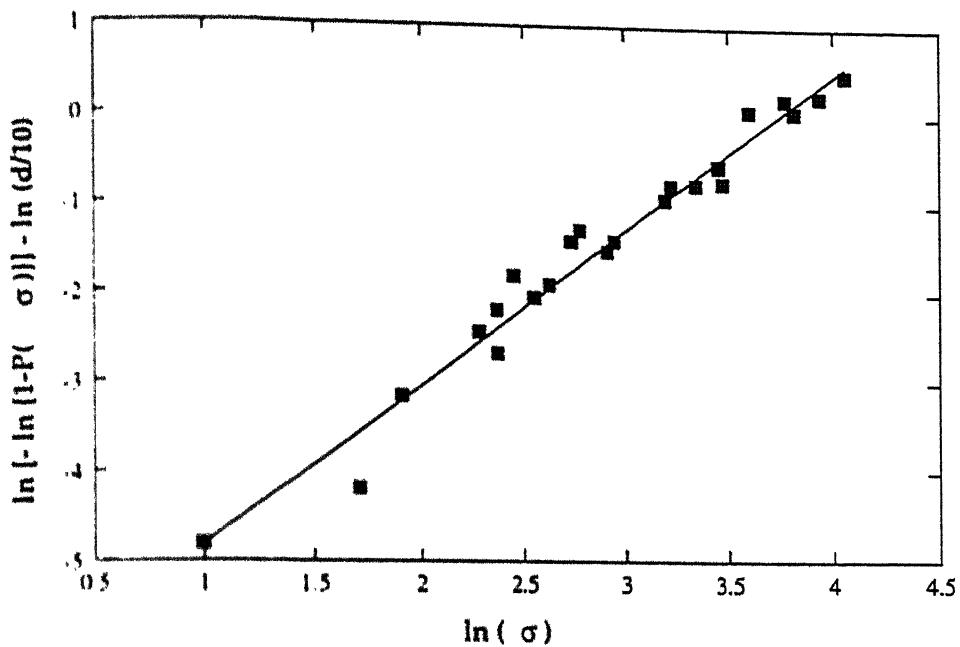
Figure 3.29: Weibull plot for 1:0.25 PZT:Fm fibres (with surface normalization)
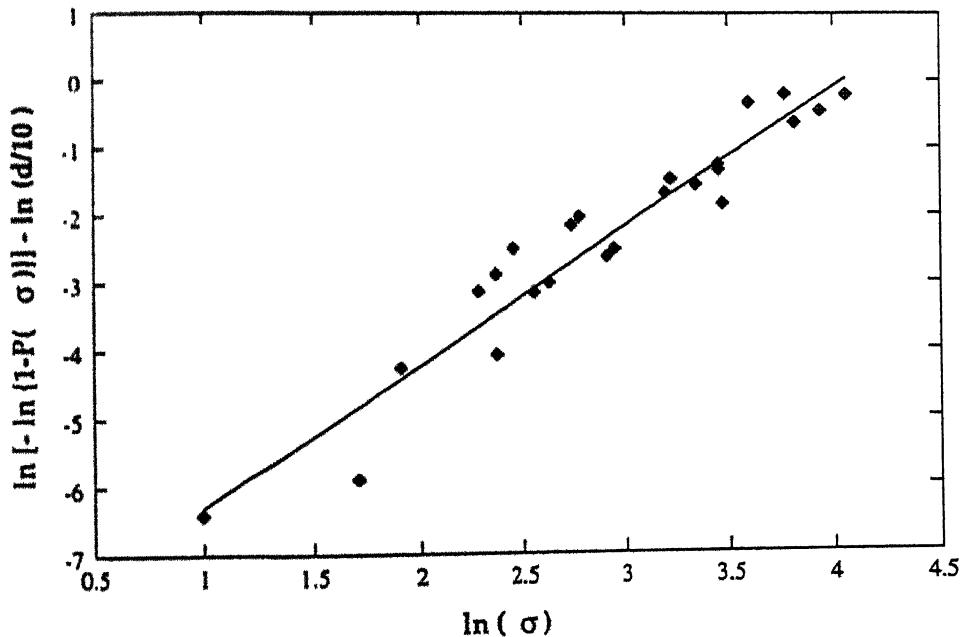
Figure 3.30: Weibull plot for 1:0.25 PZT:Fm fibres (with volume normalization)

53
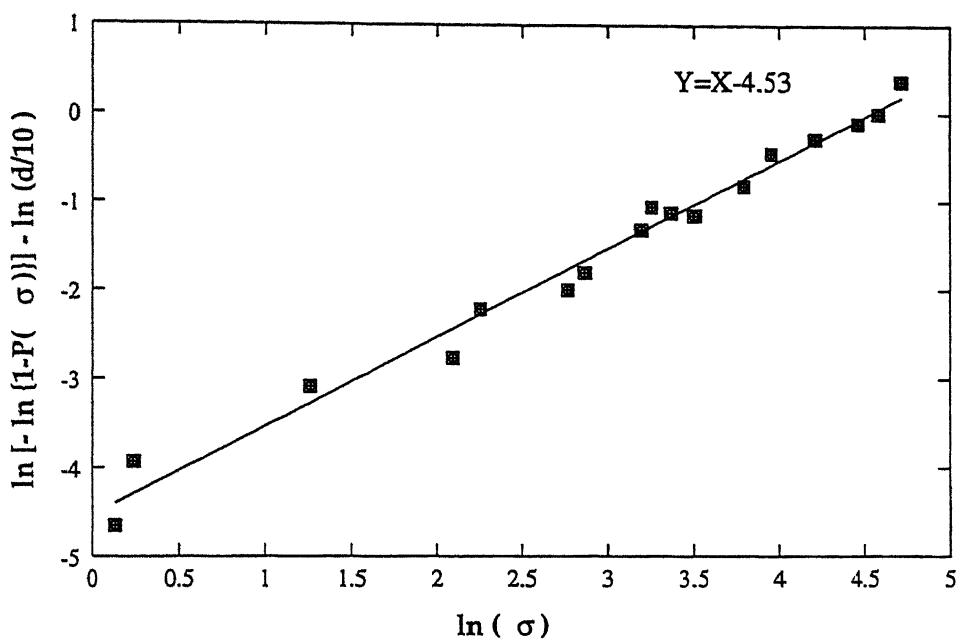
Figure 3.31: Weibull plot for 1:0.05 PZT:PEG fibres (with surface normalization)
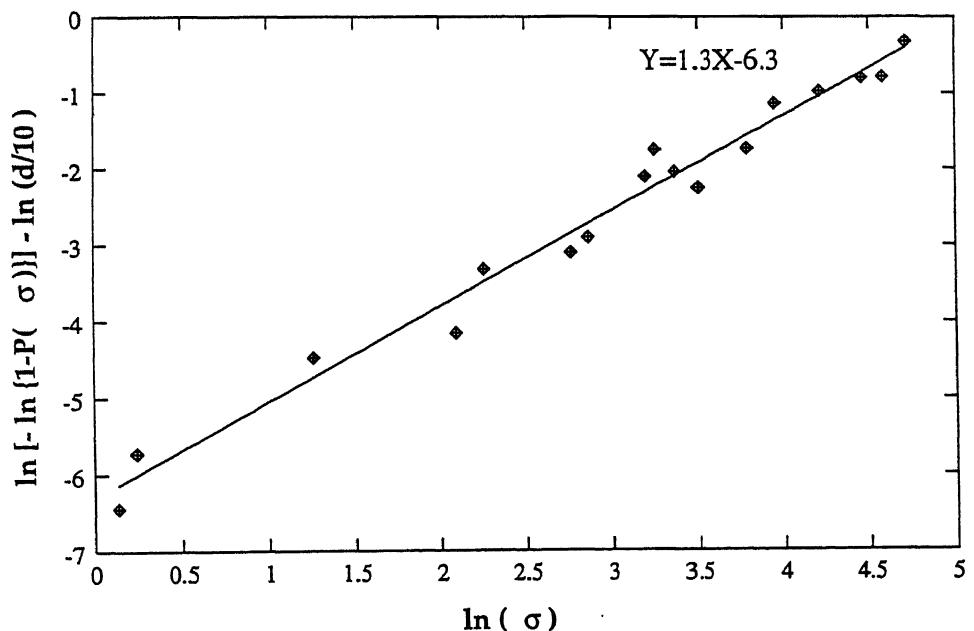
Figure 3.32: Weibull plot for 1:0.05 PZT:PEG fibres (with volume normalization)

| PZT fibres with	σ_{os}	m_s	r_s	σ_{ov}	m_v	r_v
2 mole Water	31.7	1.5	0.94	80.7	1.6	0.88
4 mole Water	40.9	2.4	0.95	64.4	2.8	0.95
0.5 mole DMF	82.8	1.4	0.96	90.5	1.8	0.95
0.25 mole DMF	50.1	1.0	0.97	83.2	1.3	0.95
0.125 mole DMF	62.0	0.9	0.99	95.7	1.2	0.98
0.5 mole Fm	25.0	1.2	0.98	44.0	1.5	0.98
0.25 mole Fm	41.3	1.8	0.99	56.2	2.1	0.96
0.125 mole Fm	40.2	1.3	0.98	57.3	1.6	0.97
0.05 m PEG-400	92.8	1.0	0.99	157.0	1.2	0.99
0.1 m PEG-400	82.0	1.4	0.99	104.4	1.6	0.98
SD7	31.9	1.1	0.98	42.8	1.5	0.98
SD20	46.5	1.0	0.98	65.4	1.4	0.99

Weibull parameter m and σ_o for sintered fibres. Subscript s, v denotes data fitted assuming surface flaws and volume flaws. Correlation coefficient is represented by r. Sample is identified by the DCCA and its molar ratio with PZT or by the drying rate.

Table 3.2: Strength of fibres
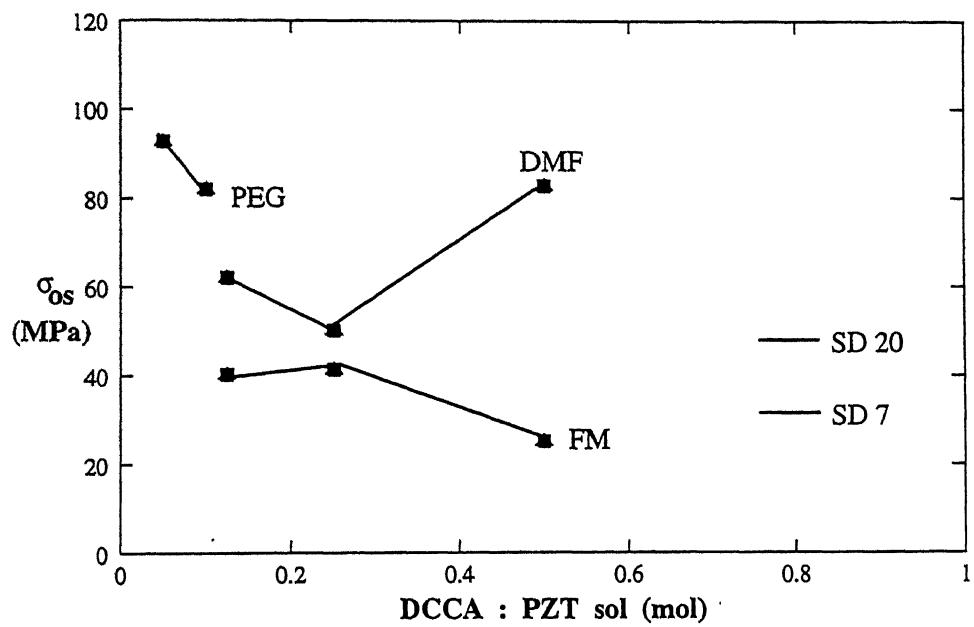
Figure 3.33: Effect of DCCA's on the strength of the fibres; the data for slow dried fibres is also shown

Chapter 4

Summary and Conclusion

4.1   Conclusion

In the present work we have tried to find out the factors responsible for the low strength of PZT fibres prepared by sol-gel process.We have tried to minimize the flaws in the fibres occuring due to removal of organics (at the time of heat treatment) by adding water to the sol to form particles. In the resulting fibres we found cracks in the cross-section which seem to increase with the amount of added water. We were successful in drawing fibres for a maximum of 4 mole of water added per mole of PZT sol. The strength value obtained seems to increase with the amount of water. We found drying cracks in the as prepared fibres and fibres heat treated at low temperature. These fibres are very fragile and their strength cannot be measured. We have tried to control the drying cracks in the fibres by using a slow drying process, and by using DCCA (DMF and Formamide) and a plasticizer PEG-400. In all the cases the fibres could be successfully drawn. The cracks in the as drawn fibres were eliminated in the slow dried fibres and in the fibres made using the DCCA. However the fibres made using PEG-400 still showed cracks at low temperatures. The strength of the as prepared fibres in all cases are very low and only few data could be obtained. Least strength seems to be obtained for the as prepared PZT fibres with PEG-400 addition.

In the sintered fibres made with PEG, the cracks found at low temperature were found to heal up. These fibres with PEG addition shows the maximum strength. Thus the strength seems to be govorned by the sintering process, and needs further investigation for improvement of the fibres.The microstructure of the sintered fibres showes different grain sizes with different additives used. Some of the interesting observations noted in our work are summerised below:

- DCCA could not be added at the begening during sol preparation as this leads to fast hydrolysis and immediate gelation giving no fibres.

- The cracking of gels could be observed as soon as gel in sealed beaker is opened to atmosphere.

- The fibre strength decreases with increase in diameter. The strength is very low for fibres above 60 μm diameter.

- Fibres with smaller diameter ($\leq$ 30 μm) after heat treatment are faint yellowish in colour and are more flexible than fibres with greater diameter. Fibres above 60 μm diameter are reddish yellow and are very brittle.

- A wide distribution in the strength data is noted.

- The strength of the as prepared fibres is very low. Upon sintering the strength is improved. Maximum strength ($\sim$90 Mpa) is obtained in fibres made using PEG.

4.2 Scope for further Research

Based on our present work we think the following research is appropiate for the improvement of PZT fibres.

- The phenomena of crack healing upon sintering in fibres using PEG should be investigated further.

- Despite our investigation the factors really responsible for low strength in the sol-gel prepared fibres are still not well understood. Perheps the main reasons are the microdisruption in the fibres due to evolution of the organics during sintering and possibly also the damage caused due to handling of the fibres. The aspect need to be investigated.

Other suggested experiments are

- Study of PZT fibres prepared with varied amount of PEG-400.

- Study of the phase formation and strength of the fibres heat treated at different temperatures.

- Prepare fibres with lower molecular weight PEG and study their properties.

- prepare fibres with longer days of slow drying.

58

- Heat treat PZT fibres in oxygen ambient for better organics removal.

- Use acidic DCCA like oxalic acid which may lead to smaller pore size distribution thus more denser product.

References

[1] P. Brack, H. Schurmans and J. Verhoest; Inorganic Fibres and Composite Materials. - A survey of recent development, *Pergamon Press*, U.K (1984)

[2] W. L. Lachman and J. P. Sterry, Chemical Eng. Progr., **58** 10, (1962) 37-41.

[3] Theodore F. Cooke, Inorganic fibres - A literature Review, *J. Am. Ceram. Soc.* **74**,12 (1991)

[4] Harold G. Sowman; A new era in ceramic fibres via sol-gel technology. *Am. Ceram. Soc. Bull.* **67** (18) (1988) 1911-1916.

[5] Toshinobu Yogo, Synthesis of polycrystalline zirconia fibre with organozirconium precursor. *J. of Mat. Science,* **25** (1990) 2394-2398.

[6] Roberto Dal Maschio, Marco Filipponi, Gian D. Soraru and Giovanni Carturan; Tensile strength of SiO_2-ZrO_2 fibres prepared by sol-gel method: Effects of preparation Artifacts and Thermal Treatments, *Am. Ceram. Soc. Bull.,* **71** (2), (1992) 204-212.

[7] B. G. Murlidharan and D. C. Agrawal, *J. of Sol-Gel Science* **9** (1997) 85-93.

[8] Kurt H. Stern.,ed., Metallurgical and Ceramic Protective Coatings. *Chapman and Hall,* London, (1997).

[9] M. W. Colly, A. Osaka, J. M. Machenjie;Effect of temperature on formation of silica gel, *J. of Non Cryst. Solids,* **82** (1986) 37-41.

[10] S.Sakka and K.Kamiya; The hydrolysis of metal alkoxides, *J. Non Cryst. Solids,* 48(1982) 31-46.

[11] C.J.Brinker and G. W. Scherer, ed, Sol-Gel Science, *Academic Press,* New York (1990).

[12] J.Zarycki, M. Prassas and J.Phalippou; *J. of Mat. Science* **17** (1982) 3371-3379.

[13] G.W.Scherer, S.A. Pardenek and R.M. Swiatek; *J. Non Cryst. Solids* **107** (1) (1988) 14-22.

[14] Larry L. Hench and Donald R. Ulrich, Science of ceramic chemical processing, *John Willey and sons,* New York. (1986) 52-64.

[15] Tatsuhiko Adachi, Sumio Sakka; Preparation of monolithic Silica gel and glass by the Sol-gel method using N,N-dimethylformamide. *J. of Mat. Science.* 22 (1987) 4407-4410.

[16] Adachi and Sakka; The role of N, N-Dimethylformamide, A DCCA, in the formation of silica gel monoliths by sol-gel method. *J. of Non-Cryst. solids* 99 (1988) 118-128.

[17] Sumio Sakka and Hiromitsu Kozzuka; Rheology of sols and Fiber drawing. *J. of Non-Cryst. solids* 100 (1988) 142-153.

[18] B. Jaffe, W. R. Cook and M. Jaffe, Piezoelectric Ceramics, *Academic Press.* London (1972)

[19] Subhasis Basu Majumdar, Phase formation, microstructural evolution, electrical and optical properties of sol-gel prepared ferroelectric PZT and Ce-PZT thin films,*Ph.D Thesis, IIT Kanpur,* (1997)

[20] Sokho Yoshikawa, Ulagaraj Selvaraj, Paul Moses, Qiyue Jiang, and Thomas Shrout; Pb(Zr,Ti)O$_3$ [PZT] fibres - Fabrication and Properties, *Ferroelectrics,* 154 (1994) 325-330.

[21] Final Report of the project "Ceramic Fibres " *Materials Science Programme,* IIT Kanpur, (1998)

[22] P.G. Lucata, Fl. Constantinescu and D.Barb, Structural dependance on sintering temperature of PZT solid solutions,*J.Am. Ceram. soc.* 64,533 (1985)

[23] D.A. Buckner and P.D. Wilcox, Effects of calcining on sintering of PZT ceramics,*Am. Ceram. Soc. Bull.,* 51,218(1972)

[24] U. Selvaraj, A.V. Prasadarao, S.Komarneni,K.Brooks, and S.K. Kurtz; *J. Mat. Reserch,* 7 (1992) 992-996.

[25] M. Guglielmi and G. Carturn; Precursors for sol-gel preparations. *J. Non Cryst. solids.* 100 (1988) 16-30.

[26] John D. Mackenzie and Donald R. Ulrich, Ultrastructure Processing of Advanced Ceramics, *John Willey and sons,* New York. (1988) 55-75.

[27] Genaro Zavala, Janos H. Fendler; Characterization of ferroelectric lead zirconate titanate films by scanning force microscopy, *J. Appl. Phys* 81 (11), (1997).

[28] Frederick E. Croxton and Dudley J. Cowden; Practical Business Statistics. *Asia Publishing House* (1961) 362-373.

[29] K. K. Phani; A new modified Weibul distribution function for the evalution of the strength of silicon carbide and alumina fibres. *J. of Mat. Science* **23** (1988) 2424-2428.

Appendix A

The C programme used for Weibull distribution analysis is given below. The data file consists of dia (μm) in the first column and strength (MPa) in the second. :

```c
#include< stdio.h >
#include< math.h >
main()
{
int i = 0, n = 0, t = 0;
float x[100], y[100];
float dd = 10 ;
float p, m_s, c_s, r_s, m_v, c_v, r_v, a, b, z, sum_x = 0,
sum_xx = 0, sum_y = 0, sum_yy = 0, sum_z = 0, sum_zz = 0, sum_xz, sum_xy = 0;
char d[10], ou[10];
void bubble();
float wbl();
FILE *fpt, *spt;
dd = wbl() ;
printf(" Enter data file name:");
scanf("%s", &d);
fpt = fopen(d,"r");
if(fpt ==0){
printf("\ nThe file "%s" does not exist in the current directory\ n", d);
exit();
}
printf("\ n Enter output file name:");
scanf("%s",&ou);
spt = fopen(ou, "w");
while(fscanf(fpt, "%f %f", &y[t], &x[t]) ! = EOF)
{
t++;
n++;
}
printf("\ n NO. OF DATA = %d\ n", n);
bubble( x , y , n);
```

```c
for(i = 0;i< = n-1;i++)
{
p = (float)(i+1)/(float)(n+1);
a = log(x[i]);
b = log(-log(1-p))-log(y[i]/dd);
z = log(-log(1-p))-2*log(y[i]/dd);
sum_x = sum_x+a;
sum_xx = sum_xx+a*a;
isum_y = sum_y+b;
sum_yy = sum_yy+b*b;
sum_z = sum_z+z;
sum_zz = sum_zz+z*z;
sum_xy = sum_xy+a*b;
sum_xz = sum_xz+a*z;
fprintf(spt, "\ n%5.5f%20.5f%30.5f", a, b, z);
}
fclose(fpt);
fclose(spt);
m_s = (sum_xy-(sum_x*sum_y/n))/(sum_xx-(sum_x*sum_x/n));
m_v = (sum_xz-(sum_x*sum_z/n))/(sum_xx-(sum_x*sum_x/n));
r_s = (n*sum_xy-sum_x*sum_y)/(sqrt(n*sum_xx-sum_x*sum_x)
sqrt(n*sum_yy-sum_y*sum_y));
r_v = (n*sum_xz-sum_x*sum_z)/(sqrt(n*sum_xx-sum_x*sum_x)
sqrt(n*sum_zz-sum_z*sum_z));

    c_s = (sum_y/n)- m_s*(sum_x/n);
c_v = (sum_z/n)- m_v*(sum_x/n);
printf("\ n(0) = %f\ n", dd);
printf("\ n_s = %f", m_s);
printf("\ n c_s = %f", c_s);
printf("\ n r_s = %f", r_s);
printf("\ n Sigma(0) = %f Mpa [Surface]", exp(-c_s/m_s));
printf("\ n\ n m_v = %f", m_v);
printf("\ n c_v = %f", c_v);
printf("\ n r_v = %f", r_v);
printf("\ n Sigma(0) = %f Mpa [Volume]", exp(-c_v/m_v));
```

```c
}

    void bubble(float x[ ], float y[ ], int n)
{
int j, pass;
float hold, ho;
int switched = 1;
for(pass = 0; pass<n-1 && switched ==1;pass++){
switched = 0;
for(j = 0; j<n-pass-1; j++)
if (x[j] >x[j+1]){
switched = 1;
hold = x[j];
ho = y[j];
x[j] = x[j+1];
x[j+1] = hold;
y[j] = y[j+1];
y[j+1] = ho;
} } }
```

A 125494

MSP-1998-M-ROY-EFF